How residual fertility impacts the efficiency of crop pest control by the sterile insect technique

Marine A Courtois, Ludovic Mailleret, Suzanne Touzeau, Louise van Oudenhove, Frédéric Grognard

HOW RESIDUAL FERTILITY IMPACTS THE EFFICIENCY OF CROP PEST CONTROL BY THE STERILE INSECT TECHNIQUE

Marine A. Courtois[1,*], Ludovic Mailleret[1,2], Suzanne Touzeau[1,2], Louise van Oudenhove[1], Frédéric Grognard[2]

[1]Université Côte d'Azur, INRAE, CNRS, ISA, France

[2]Université Côte d'Azur, Inria, INRAE, CNRS, MACBES, France

[*]Corresponding author marine.courtois@inrae.fr

Highlights

- The sterile insect technique allows pest control if not eradication.
- Pest control is possible even with residual fertility.
- Fitness costs of fertile released males matter.

Abstract

The Sterile Insect Technique (SIT) is a biological control technique based on mass-rearing, radiation-based sterilization that can induce fitness costs, and releases of the pest species targeted for population control. Sterile matings, between females and sterilized males, can reduce the overall population growth rate and cause a fall in population density. However, a proportion of irradiated males may escape sterilization, which is termed residual fertility. Our aim in this paper is to study the impact of residual fertility on pest control, by a modeling approach.

We modeled the pest population dynamics with three generic differential equations representing sterilized males, wild males and wild females. We explored the impact of residual fertility, associated or not with fitness costs, on pest control possibilities as compared to a situation in which male sterilization is flawless. We carried out a detailed mathematical analysis of the model dynamics through the computation of its equilibria and their stability. Bifurcation analyses were performed with parameters calibrated on the Mediterranean fruit fly *Ceratitis capitata*.

We showed that when residual fertility is below a threshold value, wild populations can be driven to extinction by flooding the landscape with sterilized males. This threshold is higher when residual fertility is associated with fitness costs. Too high a level of residual fertility makes SIT less effective and hinders population eradication. Nevertheless, substantial decreases in outbreak levels can still be achieved for much larger residual fertility rates.

Keywords: Modeling, Biological control, *Ceratitis capitata*, Bifurcation analysis, Ordinary differential equations, Stability analysis

1 Introduction

The Sterile Insect Technique (SIT) consists in releasing sterile males in order to decrease the number of offspring in the next generation (Dyck *et al.*, 2021). The insects of the targeted species are mass-produced, sexed (when possible) and then sterilized before being massively released in the environment. These releases dilute the population of wild males, thus the females are more likely to meet and mate with a sterile male. These matings do not produce offspring and therefore reduce the population size in the next generation.

The Sterile Insect Technique has been developed to eradicate several pests threatening human health and agriculture. Many SIT projects aim at eradicating different species of mosquitoes, vectors of numerous human diseases (Benedict, 2021). In the agricultural context, SIT has been used to eradicate the melon fly, *Bactrocera cucurbitae*, in Hawaii and the New World screw-worm fly, *Cochliomyia hominivorax*, in several places, in particular Curaçao and Mexico (Oliva *et al.*, 2022). Since its conception in the 1930s-1940s

by Knipling (1955), Bushland (Melvin and Bushland, 1936) and Serebrovsky (1940), SIT has developed rapidly and been integrated into operational area-wide integrated pest management (AW-IPM) programs (Klassen *et al.*, 2021). The range of action of the technique extends from the plot to the regional scale, to eliminate certain insects from vast territories or prevent colonization by new exotic species (Klassen and Vreysen, 2021). SIT is often associated with insect eradication programs, especially in a human epidemiological context where the objective is to eliminate the disease. However, in agriculture, instead of targeting pest eradication, the objective is to reduce pest density in order to control its economic impact.

With regard to the Mediterranean fruit fly *Ceratitis capitata*, a polyphagous dipterous insect that infects many fruit crops (Robinson and Hooper, 1989), SIT is an efficient alternative to chemical pesticides (Dunn and Follett, 2017). When mated with sterile males, females lay non-viable eggs in the fruits, thus reducing damages and increasing crop yields. This technique has been successfully deployed in several countries. Mexico and Guatemala developed the Moscamed program in 1975, joined in 1977 by the United States, to prevent the northward spread of *C. capitata* that was progressing in Central America (Enkerlin *et al.*, 2017). In 1986, the medfly was eradicated in northern Guatemala and Mexico. This success was explained by the release of billions of sterile insects on hundreds of thousands of hectares, and this for decades to avoid re-infestation. Spain has been using SIT since the 1990s (Sancho *et al.*, 2021). In France, CeraTIS-Corse is the first SIT project in an agricultural context implemented in Corsica, a French island in the Mediterranean Sea, where fruit growing is an important economic resource (Odarc, 2022).

In such programs, the deployment of SIT includes several major steps: mass production of insects, sexing (with *C. capitata*, sexing can be effectively achieved thanks to a special strain (Caceres, 2002)), sterilization and finally release of sterile insects into the environment. Sterilization is a crucial step, usually carried out through the irradiation of insect pupae with gamma rays. In many insect groups, such irradiations not only sterilize the insects, but also lead to a decrease in competitiveness (Dyck *et al.*, 2005). Indeed, it can damage many physiological processes leading to a reduction in survival, flight capacity and to the development of malformations (Guerfali *et al.*, 2011). At best, it is then necessary to release an even greater number of sterile insects to ensure the effectiveness of the technique (Robinson *et al.*, 2002). At worst, the sterile insects fail to attract and mate with wild insects, which makes the releases useless, especially for species such as *C. capitata*, in which females choose males to mate (Arita and Kaneshiro, 1985). However, the timing of irradiation can be adjusted to preserve sterilized insect competitiveness (Hooper, 1971). Indeed, insects are usually less damaged when irradiation is performed shortly after adult emergence (Estal *et al.*, 1986), but the logistic of irradiating and deploying adult flies is difficult to implement. Therefore, insects are usually irradiated at pupal stage. The irradiation dose must be as low as possible to maintain the competitiveness of sterile individuals, while maintaining the sterilization efficiency (Parker and Mehta, 2007). If the insects receive too low a dose, a significant part of them may escape sterilization. This leads to the release of fertile individuals into the environment that can be extremely damaging, as they increase the reproductive potential of the wild population and reduce the rate at which the population is suppressed (Dyck *et al.*, 2005). This proportion of non-sterile insects released is called residual fertility. The recommended sterility percentage for a SIT program is over 99.5% (FAO/IAEA/USDA, 2003). A dose inducing 100% sterility is rarely used due to the excessive damage it causes to insects (Robinson, 2005; Bakri and Mehta, 2005).

A main challenge is hence to determine how low the residual fertility rate should be to ensure pest control is achievable in the field. The question is thus to predict the residual fertility threshold, i.e. the maximal proportion of fertile irradiated males that can be accepted without threatening SIT effectiveness. Modeling represents an essential and efficient tool to tackle this issue. Indeed, modeling can guide field deployment, which is costly and time-consuming. Models of SIT have been developed for many years (Knipling, 1955; Dyck *et al.*, 2021), but only a few models focusing on *C. capitata* have been implemented (Carey, 1982; Messoussi *et al.*, 2007; Manoukis and Hoffman, 2014), and very few modeling studies have looked at residual fertility. Klassen and Creech (1971) constructed a numerical model in which a proportion of the released males remained fertile. They modified the model developed by Knipling (1955) and concluded that if the proportion of fertile males in the release is greater than the inverse of the population growth rate, the population can no longer be controlled by sterile releases. In another approach, Aronna and Dumont (2020) showed that SIT can only be successful if the residual fertility is below $1/\mathcal{R}$ where $\mathcal{R}$ is the basic reproduction number in relation to the reproductive potential of the pest population. The success of SIT is expressed as the theoretical possibility of eradicating the population by evaluating if the pest-free equilibrium is stable. This model was applied to two pest species: *Aedes albopictus* and *Bactrocera dorsalis*. A recent study focusing on *Ceratitis capitata* and examining the

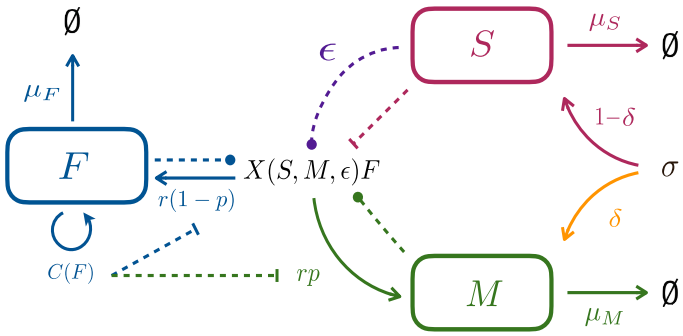

Figure 1: Flow diagram of the population dynamics model (1). The compartments (and color code) correspond to sterilized males S (pink), wild females F (blue) and wild males M (green). Solid arrows correspond to flows, dotted arrows to activating (round tip) or inhibiting effects (bar tip). Irradiated males are released at rate σ. Among these males, a proportion δ (orange) or ϵ (purple) may remain fertile, without or with associated fitness costs, respectively. Reproduction is represented by the emergence rate r, the proportion of males among offspring p, and the proportion of successful matings X. The latter increases with the density of wild males and fertile irradiated males (ϵS), but decreases with the density of sterile males. Competition among females $C(F)$ reduces the emergence rate. Finally, all compartments are affected by specific mortality rates μ.

impact of residual fertility and female re-mating, confirmed the threshold found in Aronna and Dumont (2020) for achieving population elimination (Dumont and Oliva, 2023).

In this work, we built a generic population dynamics model of SIT with sterilized males S, wild females F and wild males M compartments, from which we derived a sub-model without residual fertility and two concurrent sub-models, both incorporating residual fertiliy but with or without fitness costs associated to irradiation. In order to determine whether SIT is effective or not, bifurcation analyses were carried out to study the population control capacities associated with each sub-model. Numerical simulations were performed with parameter values specific to *C. capitata* to best account for the biology of the species.

In section 2, the general model and the residual fertility sub-models are presented. The general model is studied to determine its equilibria, their stabilities and the associated bifurcations. Section 3 is dedicated to the study of the residual fertility sub-models, calibrated with *C. capitata* parameter values, highlighting the impact of residual fertility and fitness costs. Finally, in section 4, we summarize and discuss the main results obtained.

2 Model

2.1 Model description

2.1.1 General model

The model represents the population dynamics of the following three compartments: sterilized males S, wild females F and wild males M (Fig. 1). It is defined as follows:

$$\begin{cases} \dot{S} = -\mu_S S + (1-\delta)\sigma, \\ \dot{F} = -\mu_F F + r(1-p)X(S,M,\epsilon)C(F)F, \\ \dot{M} = -\mu_M M + rpX(S,M,\epsilon)C(F)F + \delta\sigma. \end{cases} \tag{1}$$

with the dot representing time derivative.

The dynamics of sterilized males S are affected by their mortality μ_S and the release rate σ. Among σ releases, only a proportion $(1-\delta)$ of genuinely sterilized males is added to the compartment. The dynamics of wild females F are affected by their mortality μ_F and the emergence of new females. The latter is determined by the product of the emergence rate r, the proportion of females among the offspring $(1-p)$, the proportion of successful matings $X(S,M,\epsilon)$, as well as the competition between females for oviposition $C(F)$, all of it multiplied by the number of females engaged in reproduction F. Finally, the dynamics of wild males M are affected by their mortality μ_M, the emergence of new males, which is

identical to that of females up to the proportion of male offspring (complementary to that of female offspring) and a proportion of released males. Indeed, we assumed that the proportion δ of males among σ releases, that have been irradiated but remain fertile, directly contributes to the wild male population. We considered that wild individuals have a lower mortality rate than sterilized ones: $\mu_M \leq \mu_S$. Hence, fitness costs are expressed both in higher mortality and lower attractiveness.

We assumed that the proportion of successful matings $X(S, M, \epsilon)$ depends on both the density of fertile males and the density of attractive males. Fertile males correspond to wild males and a proportion ϵ of irradiated males. Attractive males correspond to wild and irradiated males, with a potential decrease in attractiveness linked to the η parameter for irradiated males. This corresponds to the biological characteristics of the species *C. capitata*, whose males aggregate and form leks in order to attract females for mating (Prokopy and Hendrichs, 1979). Thus, attractive males must be numerous enough to attract females. By being numerous and attractive, effectively sterilized males can cause a strong dilution effect, drastically reducing the number of successful matings. These biological hypotheses on the proportion of successful matings can be summarized as follows:

- $0 \leq X(S, M, \epsilon) \leq 1$
- $X(0, 0, \epsilon) = 0$
- $X(S, M, \epsilon)$ is increasing in M, concave in M and such that $\lim\limits_{M \to +\infty} X(S, M, \epsilon) = 1$

The first point signifies that X is a proportion, the second one that in the absence of males, no reproduction can take place, and the third one that the more wild males there are, the more reproduction succeeds. As an example, the proportion of successful matings can be expressed as the following function:

$$X(S, M, \epsilon) = \frac{M + \epsilon\eta S}{k + M + \eta S}. \tag{2}$$

where $k > 0$ is a constant representing the cost of being too few males and η represents the attractiveness of sterilized males. Non-zero k accounts for reduced mating at small male density linked to the associated difficulty of forming leks for *C. capitata*. In addition, we hypothesized that irradiated males suffer from a lack of attractiveness $\eta \in [0, 1]$.

The competition function $C(F)$ is a non-negative decreasing function. This feature corresponds to the competition among *C. capitata* females for oviposition (access to egg-laying sites) and thus affects the emergence rate (Papadopoulos *et al.*, 2009). Possible forms for $C(F)$ include: $\frac{1}{1+\beta F}$ which is a Beverton and Holt-like function, $e^{-\beta F}$ which is a Ricker-like function and $1 - \frac{F}{K}$ which is a logistic-like competition function, where β represents the competition strength and K the biotic capacity (Hastings and Gross, 2012). All these functions have the following characteristics:

- $C(0) = 1$ and $C(F)$ is a decreasing function
- $1/C(F)$ is convex

Among such functions, we will focus on the following explicit form:

$$C(F) = \frac{1}{1 + \beta F}. \tag{3}$$

where β represents the competition strength among females. In the model, in all cases $1/C(F)$ is strictly convex or $X(S, M, \epsilon)$ is strictly concave in M, or both.

To determine the general model equilibria and their stability in sections 2.2.1 to 2.2.3, we considered $X(S, M, \epsilon)$ and $C(F)$ satisfying the above hypotheses. For the residual fertility sub-models in section 2.1.2 and the bifurcation analysis in section 2.2.4, we chose X and C as in (2) and (3) respectively.

2.1.2 Residual fertility sub-models

In order to study the impact of residual fertility, i.e. the proportion of non-sterile irradiated males released, associated or not with fitness costs, we considered three cases extracted from general model (1).

Firstly, the case where $\delta = \epsilon = 0$ corresponds to a basic situation with no residual fertility. The explicit form of this sub-model called "Perfect sterilization" is as follows:

$$\begin{cases} \dot{S} = -\mu_S S + \sigma, \\ \dot{F} = -\mu_F F + r(1-p)\dfrac{M}{k+M+\eta S}\dfrac{1}{1+\beta F}F, \\ \dot{M} = -\mu_M M + rp\dfrac{M}{k+M+\eta S}\dfrac{1}{1+\beta F}F. \end{cases} \tag{4}$$

Secondly, we considered the existence of residual fertility without associated fitness costs. The fertile irradiated males are considered as fit as wild males in terms of attractiveness and survival, and are therefore introduced in the M compartment of the model. This case corresponds to $\epsilon = 0$ and $0 < \delta < 1$. The explicit form of this sub-model called "Cost-free residual fertility" is:

$$\begin{cases} \dot{S} = -\mu_S S + (1-\delta)\sigma, \\ \dot{F} = -\mu_F F + r(1-p)\dfrac{M}{k+M+\eta S}\dfrac{1}{1+\beta F}F, \\ \dot{M} = -\mu_M M + rp\dfrac{M}{k+M+\eta S}\dfrac{1}{1+\beta F}F + \delta\sigma. \end{cases} \tag{5}$$

And thirdly, we considered the existence of residual fertility with associated fitness costs. All irradiated males, even if they are fertile, suffer from a lack of competitiveness (i.e. attractiveness) which is represented by parameter η in the mating function, and have a higher mortality rate compared to wild males. Therefore, fertile irradiated males remain in the S compartment. This case corresponds to $\delta = 0$ and $0 < \epsilon < 1$. The explicit form of this sub-model called "Costly residual fertility" is:

$$\begin{cases} \dot{S} = -\mu_S S + \sigma, \\ \dot{F} = -\mu_F F + r(1-p)\dfrac{M+\epsilon\eta S}{k+M+\eta S}\dfrac{1}{1+\beta F}F, \\ \dot{M} = -\mu_M M + rp\dfrac{M+\epsilon\eta S}{k+M+\eta S}\dfrac{1}{1+\beta F}F. \end{cases} \tag{6}$$

These three sub-models: "Perfect sterilization" (4), "Cost-free residual fertility" (5) and "Costly residual fertility" (6), correspond to an increasing gradient of biological realism.

2.2 Model analysis

In this section, we carry out an equilibrium search and stability study on the general model (1), as the analyses on the three sub-models detailed in 2.1.2 are similar.

Under the above mentioned hypotheses the model (1) is biologically well-posed: S, F and M remain non-negative for positive time if their initial conditions are non-negative. The $\dot{S}$ equation is actually decoupled from the other two, and we assumed that S reaches its equilibrium $S^* = \frac{(1-\delta)\sigma}{\mu_S}$ very fast. Thus, we only considered the (F, M) subsystem. For readability reasons, we rewrite $X(S^*, M, \epsilon)$ as $X(M)$.

2.2.1 Reproduction numbers

From the second equation of the general model (1) with $\sigma = 0$, we have:

$$\begin{aligned} \tfrac{\dot{F}}{F} &= -\mu_F + r(1-p)X(M)C(F), \\ &\leq -\mu_F + r(1-p)\sup_M(X(M))C(0), \\ &\leq -\mu_F + r(1-p). \end{aligned}$$

This inequation is used to introduce the maximal reproduction number for females:

$$\mathcal{R}_F = \frac{r(1-p)}{\mu_F}. \tag{7}$$

$\mathcal{R}_F$ is the average number of females produced by a female during its lifetime when males M are not limiting and female competition is neglected. A necessary condition for the female population to not go extinct is that $\mathcal{R}_F$ be greater than 1.

From the third equation of (1), we have:

$$\begin{aligned}\frac{\dot{M}}{M} &= -\mu_M + rp\frac{X(M)}{M}C(F)F,\\ &\leq -\mu_M + rpX'(0)\sup_{F\geq 0}(C(F)F),\end{aligned}$$

because $X(M)$ is concave in M. This inequation allows to introduce the maximal reproduction number for males:

$$\mathcal{R}_M = \frac{rpX'(0)\sup_{F\geq 0}(C(F)F)}{\mu_M}.$$

With the explicit expressions of $X(M)$ (2) and $C(F)$ (3), we get:

$$\mathcal{R}_M = \frac{rp}{\beta k \mu_M}. \tag{8}$$

$\mathcal{R}_M$ is the average number of males produced by a male during its lifetime for the optimal number of females in the population maximizing $C(F)F$. A necessary condition for the male population to not go extinct is that $\mathcal{R}_M$ be greater than 1.

2.2.2 Equilibria

For the (F, M) subsystem at $S = S^*$, equilibria of system (1) are the solutions of the following equations:

$$\begin{cases} F(-\mu_F + r(1-p)X(M)C(F)) = 0,\\ -\mu_M M + rpX(M)C(F)F + \delta\sigma = 0.\end{cases} \tag{9}$$

Population densities at equilibrium hence verify $F^* = 0$ or $X(M^*)C(F^*) = \frac{\mu_F}{r(1-p)} = \frac{1}{\mathcal{R}_F}$ from the first equation of (9).

Pest-free equilibrium We easily deduce the pest-free equilibrium $(F^*, M^*) = (0, \frac{\delta\sigma}{\mu_M})$. When $\delta = 0$ it is a true pest-free equilibrium of the form $(0, 0)$, whereas when $\delta > 0$ the male compartment is maintained by non-sterile males within the releases.

Infestation equilibria The other equilibria must satisfy:

$$X(M)C(F) = \frac{\mu_F}{r(1-p)} = \frac{1}{\mathcal{R}_F}. \tag{10}$$

Injecting (10) into the second equation of (9), we obtain:

$$M(F) = \frac{p\mu_F}{(1-p)\mu_M}F + \frac{\delta\sigma}{\mu_M}. \tag{11}$$

Replacing M in (10) by its value in (11), we get an equation that only depends on the female density:

$$X(M(F))C(F) = \frac{1}{\mathcal{R}_F}. \tag{12}$$

As $X(M(F))$ is concave and $1/C(F)$ is convex, this equation has 2, 1 or no solutions (Appendix A). We note $G(F) = X(M(F))C(F)$ and detail these different cases below.

(i) If $G(0) < \frac{1}{\mathcal{R}_F}$ and $\max(G(F)) > \frac{1}{\mathcal{R}_F}$ (Fig. 2A) there are two solutions $F_2^* > F_1^* > 0$, such that $\frac{dG}{dF}(F_1^*) > 0$ and $\frac{dG}{dF}(F_2^*) < 0$. We then have two infestation equilibria (F_1^*, M_1^*) and (F_2^*, M_2^*).

(ii) If $G(0) > \frac{1}{\mathcal{R}_F}$ (Fig. 2B) there is only one solution, at which $\frac{dG}{dF} < 0$. This solution is named F_2^* and corresponds to the infestation equilibrium (F_2^*, M_2^*).
In the perfect sterilization case corresponding to model (4): $X(M(0)) = X(0) = 0$, so $G(0) = 0$ and this second situation cannot happen.

(iii) If $G(F) < \frac{1}{\mathcal{R}_F}$, $\forall F > 0$, there is no solution, so there is no infestation equilibrium.

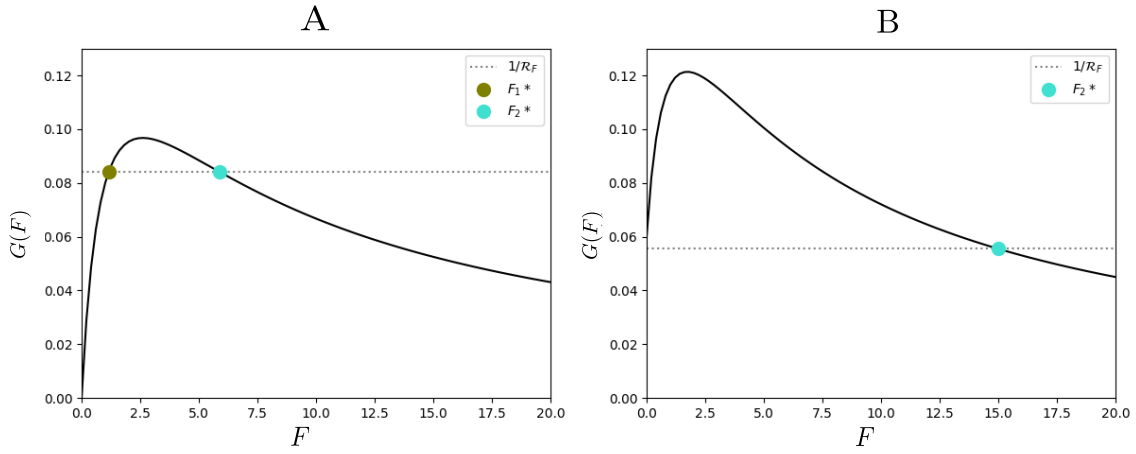

Figure 2: Female density values at the infestation equilibria of model (1). They correspond to the intersections of function $G(F)$ (in black), and the horizontal dotted line $1/\mathcal{R}_F$ (in grey). The two simulated cases correspond to different parameter values. Case A: when $G(0) < \frac{1}{\mathcal{R}_F}$ and $\max(G(F)) > \frac{1}{\mathcal{R}_F}$, there are two infestation equilibria F_1^* and F_2^*. Case B: when $G(0) > \frac{1}{\mathcal{R}_F}$, there is only one infestation equilibrium F_2^*.

2.2.3 Local stability of equilibria

We consider the Jacobian matrix of the (F, M) subsystem at $S = S^*$ of general model (1):

$$J_{(F,M)} = \begin{pmatrix} -\mu_F + r(1-p)X(M)(C'(F)F + C(F)) & r(1-p)C(F)X'(M)F \\ rpX(M)(C'(F)F + C(F)) & -\mu_M + rpC(F)X'(M)F \end{pmatrix}$$

Pest-free equilibrium At the pest-free equilibrium $(0, \frac{\delta\sigma}{\mu_M}) = (0, M(0))$:

$$J_{(0,M(0))} = \begin{pmatrix} -\mu_F + r(1-p)X(M(0)) & 0 \\ rpX(M(0)) & -\mu_M \end{pmatrix}$$

So $(0, M(0))$ is locally asymptotically stable if $X(M(0)) < \frac{1}{\mathcal{R}_F}$, i.e. $G(0) < \frac{1}{\mathcal{R}_F}$. This corresponds to cases (i) and (iii) above: there are no infestation equilibria or two infestation equilibria.

Infestation equilibria At the positive equilibria (F^*, M^*), the Jacobian is:

$$J_{(F^*,M^*)} = \begin{pmatrix} -\mu_F + r(1-p)X(M^*)(C'(F^*)F^* + C(F^*)) & r(1-p)C(F^*)X'(M^*)F^* \\ rpX(M^*)(C'(F^*)F^* + C(F^*)) & -\mu_M + rpC(F^*)X'(M^*)F^* \end{pmatrix}$$

The nullcline $r(1-p)X(M)C(F) = \mu_F$ from system (9) allows us to simplify the matrix, as follows:

$$J_{(F^*,M^*)} = \begin{pmatrix} r(1-p)X(M^*)C'(F^*)F^* & r(1-p)C(F^*)X'(M^*)F^* \\ rpX(M^*)(C'(F^*)F^* + C(F^*)) & -\mu_M + rpC(F^*)X'(M^*)F^* \end{pmatrix}$$

To determine the stability of the positive equilibria, we compute the trace and the determinant of this matrix.

For the trace, the other nullcline $rpX(M)C(F)F + \delta\sigma = \mu_M M$ from system (9), allows us to obtain:

$$J_{(F^*,M^*)} = \begin{pmatrix} r(1-p)X(M^*)C'(F^*)F^* & r(1-p)C(F^*)X'(M^*)F^* \\ rpX(M^*)(C'(F^*)F^* + C(F^*)) & -\frac{rpX(M^*)C(F^*)F^* + \delta\sigma}{M^*} + rpC(F^*)X'(M^*)F^* \end{pmatrix}$$

The computation of the trace yields:

$$\mathrm{Tr}\left(J_{(F^*,M^*)}\right) = r(1-p)X(M^*)C'(F^*)F^* - \frac{\delta\sigma}{M^*} + rpC(F^*)F^*\left(X'(M^*) - \frac{X(M^*)}{M^*}\right)$$

The first two terms are negative since $C(F)$ is decreasing. Furthermore, as $X(M)$ is concave, the last term is nonpositive. Indeed:

$$X(M^*) = X(0) + \int_0^{M^*} X'(M)dM \geq \int_0^{M^*} X'(M^*)dM = M^*X'(M^*)$$

since $X(0) \geq 0$ and $X'(M) \geq X'(M^*)$, for all $M \leq M^*$. Therefore, the trace is negative.

Regarding the determinant, we get (Appendix B):

$$\mathrm{Det}(J_{(F^*,M^*)}) = -r(1-p)\mu_M F^* \cdot \frac{dG}{dF}(F^*)$$

Therefore the sign of the slope of $G(F)$ at equilibrium determines the stability.

Exploiting the properties of F_1^* and F_2^* defined in cases (i) and (ii), we conclude that the infestation equilibrium (F_1^*, M_1^*) is unstable and (F_2^*, M_2^*) is asymptotically stable.

Summary: equilibria and local stability

(i) If $G(0) < \frac{1}{\mathcal{R}_F}$ and $\max(G(F)) > \frac{1}{\mathcal{R}_F}$, there are three equilibria: the infestation equilibrium (F_1^*, M_1^*) is unstable, while the pest-free equilibrium $(0, M(0))$ and the other infestation equilibrium (F_2^*, M_2^*) are asymptotically stable.

(ii) If $G(0) > \frac{1}{\mathcal{R}_F}$, there are two equilibria: the pest-free equilibrium $(0, M(0))$ is unstable and the unique infestation equilibrium (F_2^*, M_2^*) is asymptotically stable. This situation cannot occur for the perfect sterilization sub-model (4).

(iii) If $G(F) < \frac{1}{\mathcal{R}_F}$ for all $F \geq 0$, there is only one equilibrium, the pest-free equilibrium $(0, M(0))$, which is asymptotically stable.

2.2.4 Bifurcation diagram

The aim of this section is to determine the effect of the release rate of irradiated males σ on the long-term population dynamics. A convenient way to address this issue is to compute a bifurcation diagram. In an agricultural context, it is important to focus on the population dynamics of females, as they are the ones which cause agricultural damages. So, we chose to represent the bifurcation diagram linking the density of females F^* to the release rate σ. An expression of σ as a function of F^* was deduced from equations (10) and (12), taking explicit expressions for $X(S, M, \epsilon)$ (2) and $C(F)$ (3) described in section 2.1.1. Detailed calculations can be found in Appendix C. Thus $\sigma(F^*)$ can be expressed as follows for the general model (1):

$$\sigma(F^*) = \frac{\frac{\beta p \mu_F}{(1-p)\mu_M}(F^*)^2 + \left(\frac{p\mu_F(1-\mathcal{R}_F)}{(1-p)\mu_M} + \beta k\right)F^* + k}{\frac{\mathcal{R}_F \delta}{\mu_M} + \frac{\mathcal{R}_F \epsilon \eta(1-\delta)}{\mu_S} - \left(\frac{\delta}{\mu_M} + \frac{\eta(1-\delta)}{\mu_S}\right) - \left(\frac{\delta}{\mu_M} + \frac{\eta(1-\delta)}{\mu_S}\right)\beta F^*} \tag{13}$$

The bifurcation diagram corresponds to the locus of the points $(\sigma(F^*), F^*)$ (Fig. 3). The effect of the residual fertility can be estimated according to how parameter δ or ϵ affect the shape of this bifurcation diagram. We proceeded in two stages to study $\sigma(F^*)$: firstly, the numerator, then the denominator.

$\sigma(F^*)$ numerator The numerator is a second degree polynomial in F^* that does not depend on δ and ϵ. The roots of the numerator (F_A^* and F_B^*) then always represent the F^* equilibria for $\sigma = 0$, independently of δ and ϵ, illustrated by crosses in Fig. 3. The roots were determined classically after calculating the discriminant. We show in Appendix D that the discriminant is positive and both roots are positive when (D.20) holds ; a sufficient condition for this is that the harmonic mean of the reproduction number of females and males is greater than 4:

$$H(\mathcal{R}_M, \mathcal{R}_F) > 4.$$

It is a stronger condition than $\mathcal{R}_M > 1$ and $\mathcal{R}_F > 1$, that were identified as necessary conditions to avoid extinction of male and female populations. For this bifurcation study, we assume that this condition holds. The numerator is hence negative between F_A^* and F_B^*, positive outside.

$\sigma(F^*)$ denominator The denominator of (13) can cancel out which leads to the existence of an asymptote and several shapes for the σ bifurcation diagram. The denominator equals zero for values of F^*, named F_-^*, such that:

$$F_-^*(\delta, \epsilon) = \frac{1}{\beta}\left(\frac{\mathcal{R}_F \delta \mu_S + \mu_M \mathcal{R}_F \epsilon \eta(1-\delta)}{\delta \mu_S + \mu_M \eta(1-\delta)} - 1\right) \tag{14}$$

It can be easily shown that F^*_- is increasing in δ and ϵ. Without residual fertility ($\epsilon = 0$ or $\delta = 0$), F^*_- is negative and smaller than F^*_A. When all released males are fertile ($\epsilon = 1$ or $\delta = 1$), F^*_- goes up to $\frac{\mathcal{R}_F - 1}{\beta}$, which is larger than $F^*_A + F^*_B$ (D.21). Therefore, when the residual fertility (ϵ or δ) is large enough, F^*_- is larger than F^*_A and F^*_B. The denominator is negative above the asymptote.

Bifurcation diagram shape A bifurcation diagram of F^* as a function of the release rate σ is determined for fixed residual fertility rates. The shape of the bifurcation diagram depends on the value of the asymptote F^*_-, and in particular its position in relation to the two roots F^*_A and F^*_B of the numerator of (13). The stability of the different branches is deduced from section 2.2.3: when there are two infestation equilibria, the smaller is always unstable and the larger stable; when there is only one infestation equilibrium, it is always stable (Fig. 3). The asymptotic behavior of the model is therefore extremely dependent on both the release rate and the residual fertility of released individuals (Fig. 4).

In the perfect sterilization case, when $\delta = \epsilon = 0$ (sub-model (4)), $F^*_-(0,0) = -1/\beta$, the denominator of (13) is always negative, and the bifurcation diagrams generated has no non-negative asymptote. The sign of $\sigma(F^*)$ is the opposite of the sign of the numerator of (13) ; it is therefore positive for F^* between F^*_A and F^*_B and negative elsewhere. A similar reasoning applies for low residual fertility rates. It corresponds to shape A' in Fig. 3. With regard to stability, as the release rate σ increases, a zone of bistability precedes a zone where only the pest-free equilibrium is stable (Fig. 4).

As δ or ϵ increases so does $F^*_-(\delta, \epsilon)$, which eventually becomes positive and smaller than F^*_A; the denominator of (13) is then negative between $F^* = 0$ and F^*_-, as is the numerator. A second positive branch of $\sigma(F^*)$ thus appears between $F^* = 0$ and F^*_-, which converges from below towards a horizontal asymptote in F^*_-. $\sigma(F^*)$ remains positive between F^*_A and F^*_B. It corresponds to shape B' in Fig. 3. With regard to stability, as the release rate σ increases, three zones follow one another: a bistability zone, a zone where only the pest-free equilibrium is stable, and finally a zone where only the infestation equilibrium is stable (Fig. 4).

While δ or ϵ increases further, F^*_- gets larger than F^*_A which causes a drastic change in the bifurcation diagram. There are positive branches below F^*_A and between F^*_- and F^*_B where the numerator and denominator of (13) have the same sign, with now convergence to the asymptote from above. It corresponds to shape C' in Fig. 3. With regard to stability, as the release rate σ increases, a zone of bistability precedes a zone where only the infestation equilibrium is stable (Fig. 4).

Finally, when δ or ϵ increases even further, F^*_- gets larger than F^*_B. The positive upper branch increases now from F^*_B and converges to F^*_- from below. It corresponds to shape D' in Fig .3. With regard to stability, as the release rate σ increases, a zone of bistability precedes a zone where only the infestation equilibrium is stable (Fig. 4). This infestation equilibrium is characterized by an increase in female density as compared with a situation without releases.

It is possible to summarise the different dynamics occurring when both a component of residual fertility (ϵ or σ) and the release rate σ vary. This co-dimension 2 bifurcation diagram is sketched in Fig. 4.

3 Application to *Ceratitis capitata*

In this section, results focus on the analysis and comparison of the residual fertility sub-models presented in section 2.1.2. The parameter values used to perform the simulations were taken from the published literature and are listed in Table 1. Data and calculations related to the mortality rates, emergence rate and oviposition competition coefficient are detailed in Appendix E.

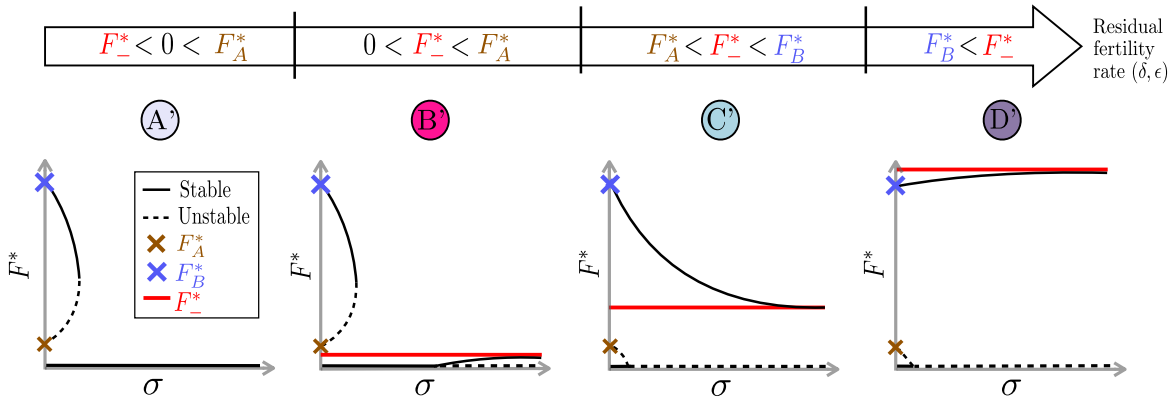

Figure 3: Qualitative σ-bifurcation diagram for sub-models with cost-free residual fertility (5) or costly residual fertility (6). The diagram, representing the density of females F^* as a function of the release rate σ, has four different shapes (A', B', C' and D') corresponding to increasing values of the residual fertility rate (δ or ϵ from 0 to 1). For sub-model with perfect sterilization (4), only shape A' applies. Stable equilibria are represented by solid lines, and unstable by dashed lines. The red line corresponds to asymptote F_-^* (14) and the crosses to the roots of the numerator of $\sigma(F^*)$ (13). These shapes do not reproduce parameter values, but are sketched manually for understanding purposes.

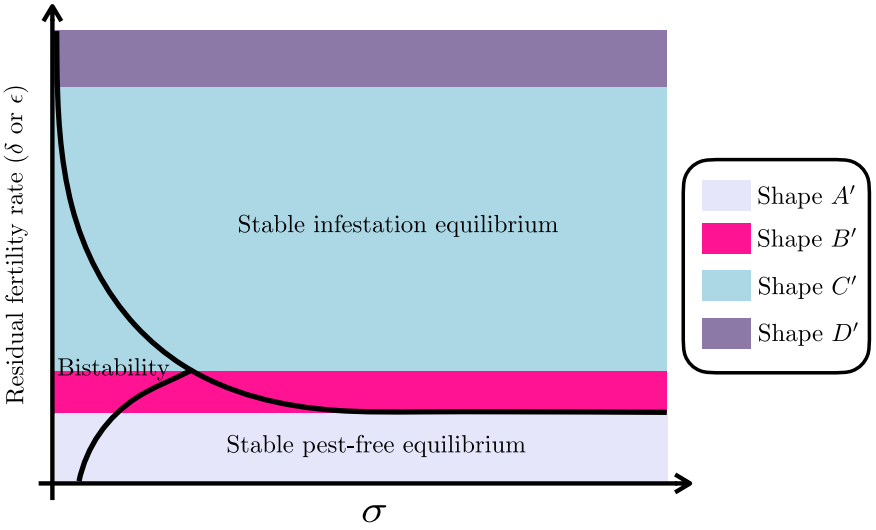

Figure 4: Stability zones as a function of the residual fertility rate δ or ϵ and the release rate σ. Three zones are defined by the black curve: the bistability zone, both the pest-free and the infestation equilibria are stable; in the other zones, only one of the two is stable. The colored areas are associated with the different shapes of bifurcation diagrams depicted in Fig. 3. The graphic was hand-drawn.

Table 1: Model parameters.

Parameters	Descriptions	Values & [Range]	Units
μ_F	Female mortality rate[1,6]	0.050 [0.018 - 0.083]	day^{-1}
μ_M	Male mortality rate[1,6]	0.036 [0.014 - 0.057]	day^{-1}
μ_S	Sterilized male mortality rate[2,6]	0.057 [0.037 - 0.077]	day^{-1}
p	Sex ratio[3]	0.500 [0.450 - 0.550]	-
r	Emergence rate[4,6]	23.7 [19.2 - 28.5]	day^{-1}
k	Mating half-saturation constant[5]	1 [0.01 - 100]	$ind.ha^{-1}$
$1-\eta$	Sterilization cost[5]	0.8 [0 - 1]	-
β	Oviposition competition between females[6]	0.24 [0.18 - 0.30]	$(ind.ha^{-1})^{-1}$
σ	Sterilized male release rate[7]	250 [0.01 - 500]	$ind.ha^{-1}.day^{-1}$
δ	Proportion of non-sterile males among the releases[7] (cost-free fertility)	0.5 [0.01 - 1]	-
ϵ	Proportion of non-sterile males among the releases[7] (costly fertility)	0.5 [0.01 - 1]	-

$ind.ha^{-1}$ corresponds to individuals per hectare.
[1] Female and male mortality rates are extracted from Vargas *et al.* (2000) and Pieterse *et al.* (2020).
[2] Sterilized male mortality rate is extracted from Juan-Blasco *et al.* (2013).
[3] Sex ratio is deduced from Juan-Blasco *et al.* (2013).
[4] Emergence rate is calculated from Pieterse *et al.* (2020).
[5] Arbitrary values.
[6] Detailed calculations in Appendix E.
[7] Studied values.

3.1 Population control capacities with SIT deployment

The ability to control pest populations can be deduced from the different shapes of bifurcation diagrams described in section 2.2.4, and thus depends on the residual fertility rate and the fitness cost associated with irradiated males.

Residual fertility impact The existence of residual fertility in the releases has a considerable impact on SIT efficiency. Without residual fertility, by adjusting the release rate σ, it is always possible to only have a stable pest-free equilibrium, and therefore to theoretically go as far as population eradication (Fig. 3, Shape A').

For very low residual fertility rates ($\delta < 5.349 \times 10^{-4}$ for sub-model (5) and $\epsilon < 4.219 \times 10^{-3}$ for sub-model (6)), Shape A' is obtained. SIT can lead to eradication of the pest population by adapting the release rate σ. Indeed, increasing σ makes it possible to move from a bistability zone, where the pest-free equilibrium but also the highest infestation equilibrium are stable, to a zone where only the pest-free equilibrium is stable (Fig. 5, purple zones).

For intermediate residual fertility rates ($5.349 \times 10^{-4} < \delta < 5.353 \times 10^{-4}$ for sub-model (5) and $4.219 \times 10^{-3} < \epsilon < 4.222 \times 10^{-3}$ for sub-model (6)), Shape B' is obtained. SIT can theoretically still lead to pest extinction. By progressively increasing σ, three different zones follow one another: first the bistability zone, then the stable pest-free equilibrium stability zone, and finally the stable infestation equilibrium stability zone (Fig. 5, tiny pink zones). In practice, this shape represents negligible fertility rate ranges as F_A^* is very close to zero.

For medium to high residual fertility rates ($5.353 \times 10^{-4} < \delta < 0.994$ for sub-model (5) and $4.222 \times 10^{-3} < \epsilon < 0.999$ for sub-model (6)), Shape C' is obtained. SIT cannot lead to the eradication of the pest population but, in the best case, to a drastic reduction in its density. Indeed, the stable infestation equilibrium zone follows the bistability zone when σ increases (Fig. 5, blue zones). However, with high sigma values, it is possible to reduce population density by more than 80% (Fig. 6). Obviously, the higher the fertility rate, the less likely it is that the population will be drastically reduced.

For even higher residual fertility rates ($\delta > 0.994$ for sub-model (5) and $\epsilon > 0.999$ for sub-model (6)), Shape D' is obtained. Population growth is enhanced by releases, which is not realistic and has therefore not been represented in this section.

So, in summary, depending on the release rate σ and the residual fertility rate, there are different zones with associated specific stabilities (Fig. 5), resulting in greater or lesser population reduction capacities (Fig. 6). Without residual fertility, by adjusting the value of the release rate it is always possible to

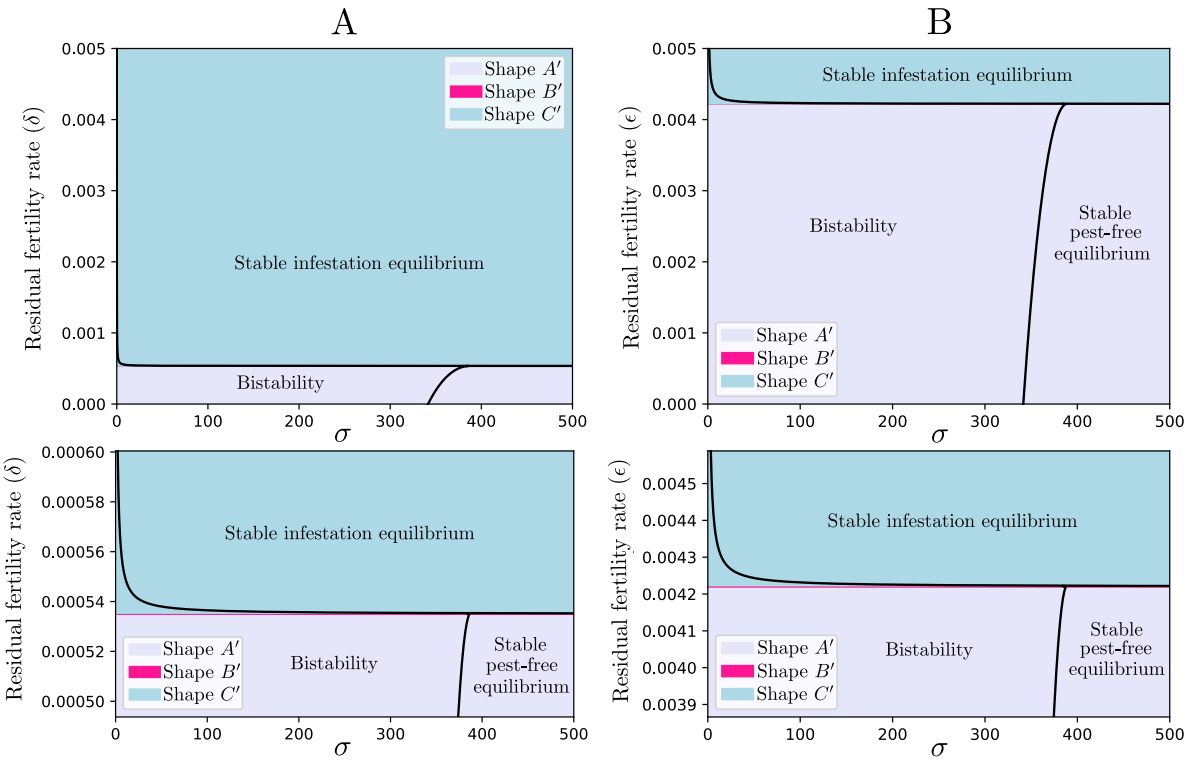

Figure 5: Stability zones as functions of residual fertility δ or ϵ and the release rate σ, for A: cost-free fertility model (5) and B: costly residual fertility model (6). The lower figures correspond to zooms of the upper figures to show the tiny pink area corresponding to Shape B'. Three zones are defined by the black curve: the bistability zone, both the pest-free and the infestation equilibria are stable; in the other zones, only one of the two is stable. The colored areas are associated with the different shapes of bifurcation diagrams depicted in Fig. 3. The scale used does not allow shape D' to be visualized.

eradicate the population, whereas with residual fertility the population can only be eradicated for a very small range of residual fertility rate values (δ or $\epsilon < 0.5\%$).

Fitness cost impact Whether there is a cost associated with the sterilization process (sub-model (6)) or not (sub-model (5)), the same four bifurcation diagram shapes are obtained (Fig. 3), but for different residual fertility rates. For example, Shape A' is obtained for higher rates for costly residual fertility compared to cost-free residual fertility (Fig. 5). In terms of population control potential, with an associated cost, the population can be reduced for higher residual fertility rates (Fig. 6). However, in both cases, when residual fertility rates are too high, population density cannot be controlled, regardless of the release rate σ. Similarly, for low σ values, population control cannot be achieved whatever the residual fertility rates.

Residual fertility thresholds to eradicate the population Shape A' (Fig. 3) is the (almost) only case for which the pest-free equilibrium can be the only stable equilibrium (shape B' being negligible), provided that the release rate is high enough (Fig. 5, purple zones). It is obtained when the asymptote F_-^*, defined in (14) is negative, which corresponds to the following residual fertility thresholds for cost-free sub-model (5):

$$\delta < \frac{\eta\mu_M}{(\mathcal{R}_F - 1)\mu_S + \eta\mu_M} = 0.001,$$

and for costly sub-model (6):

$$\epsilon < \frac{1}{\mathcal{R}_F} = 0.004. \tag{15}$$

This last result generalizes the condition obtained by Aronna and Dumont (2020) for $k = 0$.

Both thresholds are very small (less than 0.5%) and arguably hardly achievable in practice. Therefore, a more realistic goal would be to drastically reduce the population and not aim for eradication.

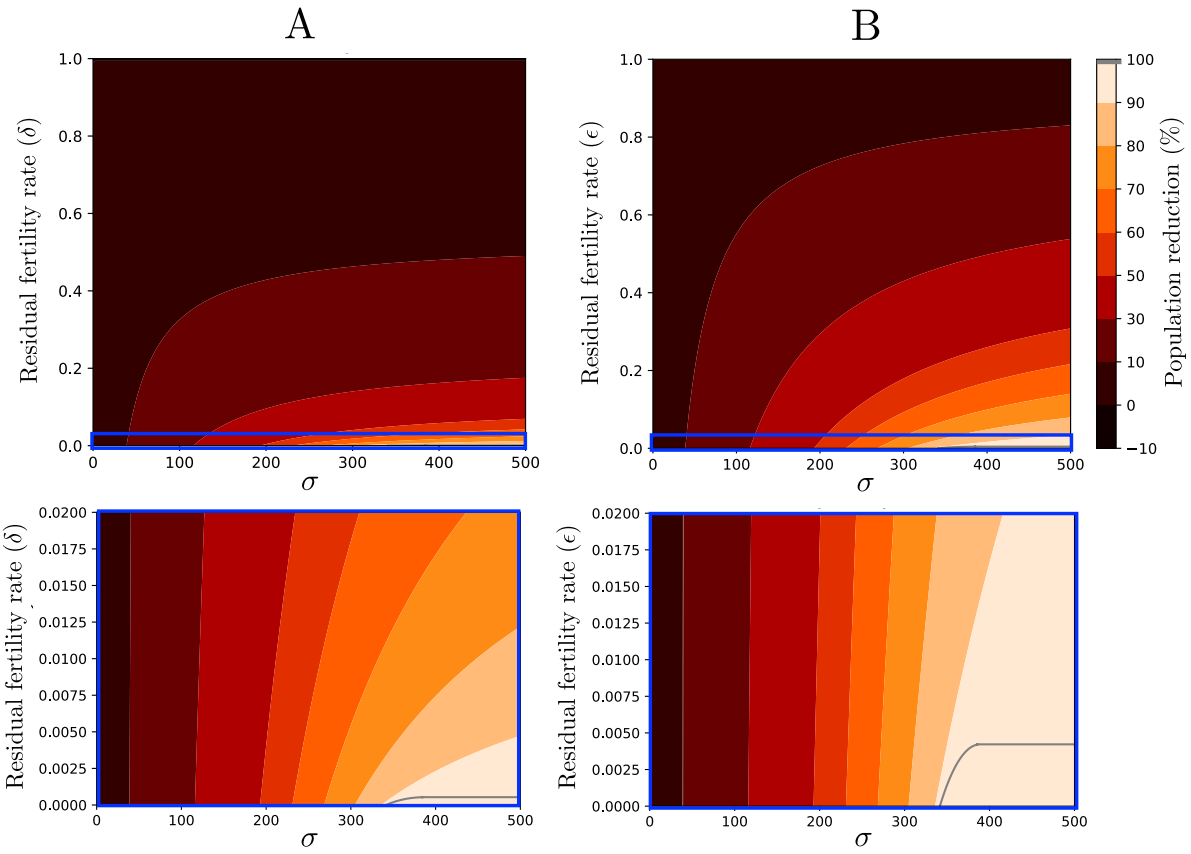

Figure 6: Contour plot illustrating the percentage of population reduction $(1-q)$, with q defined in (16), as a function of the release rate σ and the residual fertility rate, for A: cost-free residual fertility model (sub-model (5)) and B: costly residual fertility model (sub-model (6)). The lower graphs correspond to zooms of the blue boxes in the upper graphs. The grey curve visible on the zoomed-in graphs corresponds to the limit between a 90% reduction and a 100% reduction (eradication) of the population.

Residual fertility thresholds to control the population When eradication is not possible regardless of the release rate, the population reduction must be significant for the technique to be considered effective. It corresponds to shape C' (Fig. 3), in which the infestation equilibrium decreases towards the asymptote F_-^* when the release rate increases. Thus, the maximum residual fertility rate allowing a $(1-q)$ reduction of the female population density compared to the $\sigma = 0$ case is determined by solving:

$$F_-^* = qF_B^*, \tag{16}$$

For instance, a 90% population reduction corresponds to $q = 0.1$.

For the cost-free sub-model (5), we obtain:

$$\delta = \frac{(q\beta F_B^* + 1)\mu_M \eta}{\mathcal{R}_F \mu_S + (q\beta F_B^* + 1)(\mu_M \eta - \mu_S)}.$$

For a 90% female population reduction, this threshold is equal to 0.014.

Finally, for the costly sub-model (6), we obtain the following tolerable residual fertility threshold:

$$\epsilon = \frac{1}{\mathcal{R}_F} + \frac{qF_B^*\beta}{\mathcal{R}_F}. \tag{17}$$

The threshold for population control is thus $\frac{qF_B^*\beta}{\mathcal{R}_F}$ higher than the threshold required for population eradication, it is equal to 0.103.

For the particular case where $k = 0$, we obtain:

$$\epsilon = \frac{1}{\mathcal{R}_F} + q(1 - \frac{1}{\mathcal{R}_F}), \tag{18}$$

so that for a 90% female population reduction, this threshold is equal to 0.104.

Convergence time To optimize the effectiveness of SIT, it is essential to consider not only the residual fertility rate, but also the release rate σ. In Fig. 6, for a given residual fertility rate, a range of σ values will lead to the same population reduction range. However, σ has an influence on the convergence time to reach a given population reduction range, so that higher σ values allow for faster population control. For example, a release rate σ ten times higher allows to reach extinction or population reduction much faster for all sub-models (Fig. 7): 75 days are enough for the higher release rate, but it takes between 200 and 300 days for the lower rate to get close to the equilibrium value, starting from the uncontrolled infestation equilibrium.

3.2 Sensitivity analysis

A global sensitivity analysis was performed to determine the most influential parameters on percentage of female population reduction $(1-q)$, with q defined in (16), in order to study how to improve pest population control.

We used a variance-based method (Sobol, 1990; Wu *et al.*, 2013). For each parameter, three values were tested, corresponding to the reference value, plus the minimum and maximum values of the range specified in Table 1). A full factorial design was used to explore the parameter space. An ANOVA was then performed to obtain the variance decomposition based on a linear model with two-way interactions between the output and the parameters. Finally, Sobol Sensitivity Indices (SI) and Total Sensitivity Indices (TSI) were calculated for each parameter as follows: the SI as the ratio between the sum of squares of the parameter main effect and the total sum of squares; the TSI as the ratio between the sum of squares of the parameter main effect plus its interactions and the total sum of squares.

The parameter with the greatest influence on female density reduction is the female mortality rate μ_F with a total sensitivity index greater than 50% (Fig. 8). The competition coefficient between females β and the emergence rate r, which both relate to the biology of the species, also have a significant influence. Finally, parameters directly related to SIT - the residual fertility rate (δ or ϵ), the release rate σ and the cost of sterilization η - also have a major influence on female density reduction. The other parameters, i.e. male and sterilized male mortality rates (μ_M and μ_S) and the mating half-saturation constant k, have a negligible influence compared to the others.

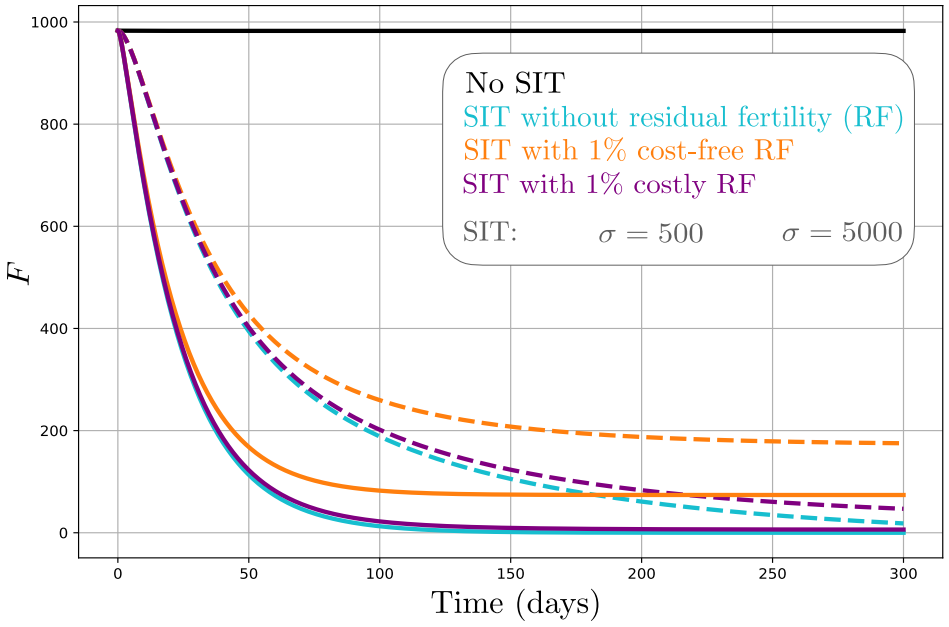

Figure 7: Temporal simulations of female population dynamics (F). Four cases are considered: no SIT (black curve), SIT without residual fertility (blue curves), SIT with 1% cost-free residual fertility (orange curves) and SIT with 1% costly residual fertility (purple curves). The dotted curves were obtained with the release rate $\sigma = 500$ ind.ha^{-1}.day^{-1} and the solid curves with $\sigma = 5000$ ind.ha^{-1}.day^{-1}.

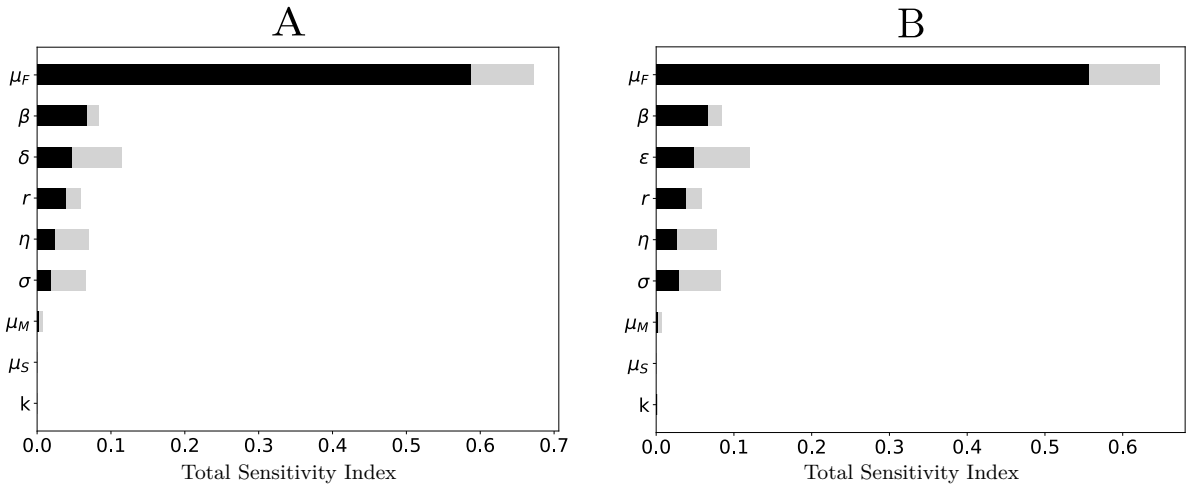

Figure 8: Total sensitivity index per parameter, separated into main effect (black bar, SI) and two-way interactions (grey bar). Sensitivity analysis performed on female density reduction for A: cost-free residual fertility sub-model (5) and B: costly residual fertility sub-model (6).

4 Discussion

We investigated the impact of residual fertility on sterilized male release efficiency in the context of SIT deployment. We showed that, as hypothesized, imperfect sterilization has a significant impact on the effectiveness of SIT. In addition, when a fitness cost is associated with radiation exposure, higher residual fertility rates can be tolerated to achieve effective control of the pest. The analysis carried out shows the impact of residual fertility, and emphasizes the need to better understand the sterilization and release process. Indeed, the fertile released males threaten more the effectiveness of SIT if they present the same phenotypic and behavioral traits as the wild males (cost-free sub-model), rather than when they share their characteristics with the sterilized males (costly sub-model). This analysis shows that it is capital to apprehend the mechanisms underpinning the residual fertility and to understand how the males escaping sterilization are impacted by the different SIT processes (mass-breeding, irradiation, transport and release). Have the irradiated males lost their fitness but have some conserved viable sperm? Or have some males escaped the sterility-inducing rays and retained all their fitness? In a nutshell, our results illustrate the importance of considering not only the sterilized male release rate required to reduce the population density in a timely manner, but also the residual fertility rate and associated fitness costs.

In our study, costs were associated with irradiated males at two levels: firstly, sterilized males had a higher mortality than wild-type males and secondly, a lower mating rate (parameter η). The latter can be due to reduced attractiveness, flight and dispersal capacity (Guerfali *et al.*, 2011), or limited competitiveness (Dyck *et al.*, 2005). The dose needed to induce total sterility in *C. capitata* induces a significant drop in male performance (Robinson *et al.*, 2002), so SIT programs rarely aim at 100% sterility (Parker and Mehta, 2007) and the addition of aromatherapy based on ginger root oil, known to improve the attractiveness of sterile males, is often adopted (Morelli *et al.*, 2013). Aromatherapy has been confirmed as an essential step in the success of SIT against *C. capitata* (Dumont and Oliva, 2023). In this species, the attractiveness of sterilized males is indeed essential, as males gather in leks (Whittier *et al.*, 1992), to court wild females, attract them and finally mate (Shelly and McInnis, 2016). According to our sensitivity analysis, the influence of this η cost on the reduction of population density is significant, which highlights the importance of determining the traits affected by the sterilization process and of quantifying their impact on the male mating capacity. In contrast, the mortality rate of sterilized males, linked to the radiation dose they received, does not have a major influence. This point illustrates the complexity of the trade-off between radiation dose and fitness, and hence competitiveness of irradiated males. Other authors addressed this trade-off issue and suggested that lower doses than those applied to achieve high sterilization rates can optimize SIT, noting that any increase in residual fertility is more than offset by the increased competitiveness of the released insects (Parker and Mehta, 2007). In our study, the sensitivity analysis shows that residual fertility rate (δ or ϵ) has a similar if slightly higher impact on SIT effectiveness compared to sterilization cost ($1-\eta$), which suggests that increased residual fertility rates could be mitigated by increased irradiated male competitiveness. Other species-specific parameters had a significative influence on population reduction: they were either linked to density-dependence processes (e.g. competition strength) or population growth (e.g. fertility and emergence rate). This underlines the importance of understanding both qualitatively and quantitatively the demographic processes driving the pest population dynamics.

The objective of SIT programs in the agricultural context is to reduce fruit damages, and therefore population levels, below an economic damage threshold (Dyck *et al.*, 2021). This study confirms that the effectiveness of SIT depends largely on the residual fertility rate in the releases (Dyck *et al.*, 2005; Parker and Mehta, 2007; Dumont and Oliva, 2023). The lower the residual fertility rate, the more effective the control. In the majority of theoretical studies, the effectiveness of SIT is associated with a stable pest-free equilibrium and thus with the possibility of eradicating the population (Bliman *et al.*, 2019; Aronna and Dumont, 2020). As Aronna and Dumont (2020), we show that the threshold allowing population eradication in the costly sub-model is $1/\mathcal{R}_F$ (15), which is less than 0.5%. It is even lower for the cost-free residual fertility sub-model. Hence, the possibility of eradicating the population exists only for very low residual fertility rates. However, even if eradication is theoretically impossible, it does not mean that control is impossible and that the technique is useless. Indeed, in the South African SIT program against *C. capitata*, the objective was to bring fly populations below an economic threshold and then create an internationally recognised low pest prevalence area (Zavala-López and Enkerlin, 2017). This can be achieved when the pest-free equilibrium is stable, but also when it is unstable and a low pest equilibrium is stable. Thus, we show that a residual fertility threshold $\frac{1}{\mathcal{R}_F} + \frac{qF_B^*\beta}{\mathcal{R}_F}$ (17), higher than the eradication threshold, is theoretically acceptable to control the population. We showed that, up to this threshold of 10% of residual fertility, the population can be reduced by $1-q = 90\%$ of the uncontrolled equilibrium

density. This 90% reduction would indeed be acceptable as it would bring the amount of males caught by 50 traps over an hectare from 982, at the uncontrolled equilibrium density, down to 98 which is below the economic threshold of about 3 males per trap and per day for *C. capitata* (Hafsi *et al.*, 2020a). Thus, efficiently deploying this technique does not necessarily require the eradication of the species in the area of interest, where the persistence of a low population density causes negligible economic losses.

With a residual fertility threshold of 1%, which is the typical threshold for *C. capitata*, the IAEA recommends releasing about 4000 individuals per week and per hectare. Our results suggest, for a costly residual fertility of 1%, that a release of about 400 sterilized males per day per hectare would be sufficient to control the population (at least 90% reduction in Fig. 6), which corresponds to $2,800$ males per week and per hectare. So, our model allows us to estimate release rates of the same order of magnitude as those recommended for *C. capitata*. According to our model, for a cost-free residual fertility of 1%, a release of more than $8,000$ males per week and per hectare would be necessary to ensure a 90% population reduction. If fertile released males are as fit as wild males, our results show that the releases should be more than twice the IAEA recommendations. Therefore, release recommendations should not only take into account residual fertility but also the fitness of released individuals.

By studying residual fertility, we are considering the possibility of introducing fertile irradiated males into the environment, which raises ethical and safety issues (Oliva *et al.*, 2021). With current IAEA recommendations, the risk that residual fertility might compromise pest population control is fairly low. However, the release of non-sterile irradiated males raises issues relative to the introduction of non endemic strains into a wild population (Lynch and Thomas, 2000; Benedict *et al.*, 2018). Indeed, non-sterile males can reproduce and transfer their genes, potentially introducing new alleles and new phenotypes into the target population. Moreover, strains used for releases in the SIT context might be different from wild population in many regards. First, strains might be genetically selected to choose specific properties, such as the developing of genetic sexing traits (Robinson, 2002; Ramírez-Santos *et al.*, 2016). Second, mass rearing during many generations has probably lead to adaptation to laboratory conditions (Hoffmann and Ross, 2018). And third, individuals are irradiated to induce sterilization, which can lead to numerous unknown mutations. Residual fertility is thus a threat to SIT programs in the sense that it makes self-replication possible, making sterile insects comparable to other biocontrol agents (Kapranas *et al.*, 2022). Indeed, crosses between introduced and local biocontrol agents are possible, making hybrids with non-controlled traits that potentially increase the risk of invasion (Turgeon *et al.*, 2011). The context of SIT is generally comparable to inundation biological control (mass introduction of macro-organisms (Eilenberg *et al.*, 2001)), because (i) the released species is already established in the target area (since it is the target species) and (ii) sterile insects are mass released. In inundation or classical biological control, the main non-target effects concern the risk that the introduced biocontrol agents attack other species than the target pest (Lynch and Thomas, 2000). SIT is based on intra-specific competition between the released and the wild males and is thus highly specific to the target species (Abram *et al.*, 2021). Residual fertility might thus lead to two different non-target effect: (i) when SIT is used preventively against a species not present in the target area, it might promote its earlier establishment (Kapranas *et al.*, 2022), and (ii) it might allow gene flow between introduced individuals and wild populations. To our knowledge, no gene flows have been observed (or studied) following the release of sterile insects but further studies might be necessary for quantitative risk assessment (David *et al.*, 2013; Kapranas *et al.*, 2022).

The model's bistability cases show that with low release rates, it is possible to control a population quickly if the initial conditions are not too high, i.e. below the unstable equilibrium. This is why SIT is particularly effective at low population densities. In order to achieve effective population control, the idea is either to start releases particularly early, before the strong invasion phase of the pest, or to combine with other control methods to reduce densities beforehand. The most obvious method is prophylaxis, i.e. all measures designed to prevent the arrival of the pest in the crop or greatly reduce its outbreak, thus limiting the size of the pest population even before the implementation of SIT (Benedict, 2021). For fruit flies such as *C. capitata*, crushing fallen fruits and ploughing the soil over winter to expose pupae to moisture, frost and predators can be effective prophylactic measures. SIT is often part of area-wide integrated pest management programs, in which the technique is used in combination with pesticides (Vreysen *et al.*, 2006). Indeed, pesticides can help to reduce population densities before the start of releases, but they have a detrimental effect on sterilized males released, problems of resistance in *C. capitata* have been reported (Magaña *et al.*, 2007) and the current aim is to reduce their use. So, to eliminate a part of pests without using pesticides, SIT can be considered in combination with trapping. However, this option is subject to debate. Indeed, some authors claim that for *C. capitata*, mass trapping in a limited area is compatible with SIT without requiring an increase in release effort (Duarte *et al.*, 2022). On the one hand, if the traps preferentially attract males (Leza *et al.*, 2008), whether wild or

sterile, they will be trapped, thus maintaining the proportion of wild and sterile males and preserving SIT effectiveness. On the other hand, it seems ineffective to release sterilized males doomed to be captured. So, for effective pest population control, theoretical study of this option may represent a real challenge, in order to have a prior idea of the effectiveness associated with the trap deployment effort to be envisaged.

5 Data accessibility and reproductibility

All analyses were performed using the Python programming language (version 3.11.0). The complete script coded in Python, specifying the versions of the libraries used, is available on the following link: https://gitlab.com/marinecourtoism2/sit_residual_fertility.

A Existence of equilibria

The infestation equilibria are the solutions of $G(F) = X(M(F))C(F) = \frac{1}{\mathcal{R}_F}$ (12) for the female density, from which the male density is deduced using (11). Equilibria thus correspond to intersections between the curves $X(M(F))$ and $\frac{1}{\mathcal{R}_F C(F)}$. The first being concave and the second convex, there can be 2, 1 or 0 infestation equilibria.

In order to study the derivative of $G(F)$ (12) we first note that:

$$\frac{d}{dF}\left[\left(X(M(F)) - \frac{1}{\mathcal{R}_F C(F)}\right) C(F)\right] = \frac{d}{dF}\left(X(M(F)C(F))\right).$$

Developing the derivative in the square brackets, we have:

$$\frac{d}{dF}\left[\left(X(M(F)) - \frac{1}{\mathcal{R}_F C(F)}\right) C(F)\right] = \frac{d}{dF}\left(X(M(F)) - (\frac{1}{\mathcal{R}_F C(F)})\right) C(F) + \left(X(M(F)) - \frac{1}{\mathcal{R}_F C(F)}\right) \frac{d}{dF} C(F).$$

Merging the two equations and noting that at equilibrium $X(M(F^*)) = \frac{1}{\mathcal{R}_F C(F^*)}$, we obtain:

$$\frac{d}{dF}(X(M(F)C(F)) = \left(\frac{d}{dF}(X(M(F)) - \frac{d}{dF}\left(\frac{1}{\mathcal{R}_F C(F)}\right)\right) C(F).$$

As $C(F) > 0$, the sign of the derivative of $X(M(F))C(F)$ depends on the sign of the difference between the derivatives of $X(M(F))$ and $\frac{1}{\mathcal{R}_F C(F)}$. The difference is non-negative for the first equilibrium called F_1^* (when it exists) as $X(M(F)) < \frac{1}{\mathcal{R}_F C(F)}$ for $F < F_1^*$, the reverse is true for F_2^* (Fig. A.1). From the concavity and convexity conditions, this non-negativity, respectively non-positivity, turns positive, respectively negative (Fig. A.1).

Thus, when $\frac{d}{dF}X(M(F)) > \frac{d}{dF}\left(\frac{1}{\mathcal{R}_F C(F)}\right)$, we have $\frac{dG}{dF}(F^*) > 0$ as $X(M(F)C(F) = G(F)$, it corresponds to F_1^* ; and when $\frac{d}{dF}X(M(F)) < \frac{d}{dF}\left(\frac{1}{\mathcal{R}_F C(F)}\right)$, we have $\frac{dG}{dF}(F^*) < 0$, it corresponds to F_2^*.

To sum up:

(i) If the curves intersect at two positive points (Fig. A.1A): there are two solutions $F_2^* > F_1^* > 0$, such that $\frac{dG}{dF}(F_1^*) > 0$ and $\frac{dG}{dF}(F_2^*) < 0$. We then have two infestation equilibria (F_1^*, M_1^*) and (F_2^*, M_2^*).

(ii) If the curves intersect at one positive point only (Fig. A.1B): there is only one solution, at which $\frac{dG}{dF} < 0$. This solution is named F_2^* and corresponds to the infestation equilibrium (F_2^*, M_2^*).

(iii) If there is no intersection between the curves: there is no solution, so there is no infestation equilibrium.

B Determinant computation

In this section, the calculation of the determinant of the Jacobian matrix defined in section 2.2.3 is detailed. As a reminder, the Jacobian matrix $J_{(F^*,M^*)}$ is expressed as follows:

$$J_{(F^*,M^*)} = \begin{pmatrix} -r(1-p)X(M^*)C(F^*) + r(1-p)X(M^*)(C'(F^*)F^* + C(F^*)) & r(1-p)C(F^*)X'(M^*)F^* \\ rpX(M^*)(C'(F^*)F^* + C(F^*)) & -\mu_M + rpC(F^*)X'(M^*)F^* \end{pmatrix}.$$

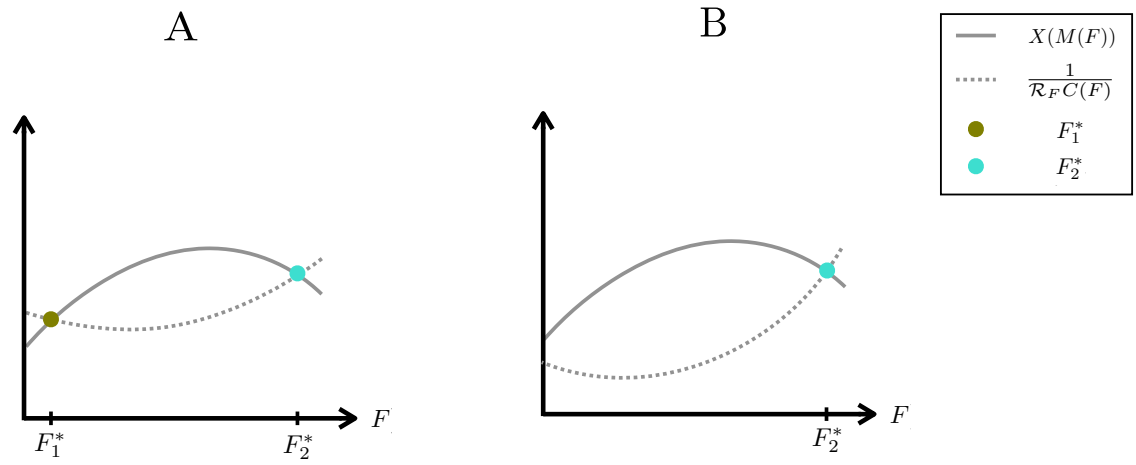

Figure A.1: Female density values at the infestation equilibria of the model (1). They correspond to the intersections between concave curve ($X(M(F))$ (grey solid line) and convex curve $\frac{1}{\mathcal{R}_F C(F)}$ (grey dotted line). Curves were sketched by hand. In case A, there are two infestation equilibria F_1^* (green point) and F_2^* (blue point). In case B, there is only one infestation equilibrium F_2^* (blue point).

The determinant is calculated as follows:

$$\begin{aligned}
Det(J(F^*,M^*)) &= r(1-p)X(M^*)C'(F^*)F^*(-\mu_M + rpC(F^*)X'(M^*)F^*) \\
&\quad - r(1-p)C(F^*)X'(M^*)F^*rpX(M^*)(C'(F^*)F^* + C(F^*)), \\
&= r(1-p)F^*[X(M^*)C'(F^*)(-\mu_M + rpC(F^*)X'(M^*)F^*) \\
&\quad - C(F^*)X'(M^*)rpX(M^*)(C'(F^*)F^* + C(F^*))], \\
&= r(1-p)F^*[-\mu_M X(M^*)C'(F^*) - C(F^*)X'(M^*)rpX(M^*)C(F^*)], \\
&= r(1-p)F^*\left[-\mu_M X(M^*)C'(F^*) - C(F^*)X'(M^*)\tfrac{p\mu_F}{(1-p)}\right],
\end{aligned}$$

as $X(M^*)C(F^*) = \frac{\mu_F}{r(1-p)}$ (10). In addition, according to (11), $M'(F^*) = \frac{p\mu_F}{(1-p)\mu_M}$, so the determinant can be written:

$$\begin{aligned}
Det(J(F^*,M^*)) &= -r(1-p)\mu_M F^*\left[(X(M^*)C'(F^*) + \tfrac{p\mu_F}{(1-p)\mu_M})C(F^*)X'(M^*)\right], \\
&= -r(1-p)\mu_M F^*\left[X(M^*)C'(F^*) + M'(F^*)C(F^*)X'(M^*)\right], \\
&= -r(1-p)\mu_M F^*\tfrac{dG}{dF}(F^*),
\end{aligned}$$

as $X(M^*)C'(F^*) + X'(M^*)M'(F^*)C(F^*) = \frac{dG}{dF}(F^*)$.
Thus, the sign of the determinant is equal to the sign of the slope of $G(F)$ at the equilibrium.

C $\sigma(F^*)$ expression

In this section, the calculations leading to the explicit expression of $\sigma(F^*)$ (13) are detailed. In equation (12), we substitute $X(S,M,\epsilon)$ by explicit expression (2) and obtain:

$$(12) \iff \frac{M(F^*)+\epsilon\eta S^*}{k+M(F^*)+\eta S^*}\cdot C(F^*) = \frac{1}{\mathcal{R}_F}.$$

Substituting $S^* = \frac{(1-\delta)\sigma}{\mu_S}$ and $M(F^*) = \frac{p\mu_F}{(1-p)\mu_M}F^* + \frac{\delta\sigma}{\mu_M}$ from equation (11), we then obtain:

$$
\begin{aligned}
&\iff \frac{\frac{p\mu_F}{(1-p)\mu_M}F^* + \frac{\delta\sigma}{\mu_M} + \frac{\epsilon\eta(1-\delta)\sigma}{\mu_S}}{k + \frac{p\mu_F}{(1-p)\mu_M}F^* + \frac{\delta\sigma}{\mu_M} + \eta\frac{(1-\delta)\sigma}{\mu_S}} \cdot C(F^*) = \frac{1}{\mathcal{R}_F},\\
&\iff \frac{\mathcal{R}_F p\mu_F}{(1-p)\mu_M}F^* + \frac{\mathcal{R}_F\delta\sigma}{\mu_M} + \frac{\mathcal{R}_F\epsilon\eta(1-\delta)\sigma}{\mu_S} = \frac{1}{C(F^*)}\left(k + \frac{p\mu_F}{(1-p)\mu_M}F^* + \frac{\delta\sigma}{\mu_M} + \eta\frac{(1-\delta)\sigma}{\mu_S}\right),\\
&\iff \frac{\mathcal{R}_F\delta\sigma}{\mu_M} + \frac{\mathcal{R}_F\epsilon\eta(1-\delta)\sigma}{\mu_S} - \frac{1}{C(F^*)}\frac{\delta\sigma}{\mu_M} - \frac{1}{C(F^*)}\left(\eta\frac{(1-\delta)\sigma}{\mu_S}\right) = \frac{1}{C(F^*)}\left(k + \frac{p\mu_F}{(1-p)\mu_M}F^*\right) - \frac{\mathcal{R}_F p\mu_F}{(1-p)\mu_M}F^*,\\
&\iff \sigma\left(\frac{\mathcal{R}_F\delta}{\mu_M} + \frac{\mathcal{R}_F\epsilon\eta(1-\delta)}{\mu_S} - \frac{1}{C(F^*)}\frac{\delta}{\mu_M} - \frac{1}{C(F^*)}\left(\eta\frac{(1-\delta)}{\mu_S}\right)\right) = \frac{1}{C(F^*)}\left(k + \frac{p\mu_F}{(1-p)\mu_M}F^*\right) - \frac{\mathcal{R}_F p\mu_F}{(1-p)\mu_M}F^*,\\
&\iff \sigma(F^*) = \frac{\left(\frac{1}{C(F^*)}\right)\left(k + \frac{p\mu_F}{(1-p)\mu_M}F^*\right) - \frac{\mathcal{R}_F p\mu_F}{(1-p)\mu_M}F^*}{\frac{\mathcal{R}_F\delta}{\mu_M} + \frac{\mathcal{R}_F\epsilon\eta(1-\delta)}{\mu_S} - \frac{1}{C(F^*)}\frac{\delta}{\mu_M} - \frac{1}{C(F^*)}\left(\eta\frac{(1-\delta)}{\mu_S}\right)}.
\end{aligned}
$$

By expliciting $C(F^*)$ using expression (3), we have:

$$
\begin{aligned}
\sigma(F^*) &= \frac{(1+\beta F^*)\left(k + \frac{p\mu_F}{(1-p)\mu_M}F^*\right) - \frac{\mathcal{R}_F p\mu_F}{(1-p)\mu_M}F^*}{\frac{\mathcal{R}_F\delta}{\mu_M} + \frac{\mathcal{R}_F\epsilon\eta(1-\delta)}{\mu_S} - (1+\beta F^*)\frac{\delta}{\mu_M} - (1+\beta F^*)\left(\eta\frac{(1-\delta)}{\mu_S}\right)},\\
&= \frac{\frac{\beta p\mu_F}{(1-p)\mu_M}(F^*)^2 + \left(\frac{p\mu_F(1-\mathcal{R}_F)}{(1-p)\mu_M} + \beta k\right)F^* + k}{\frac{\mathcal{R}_F\delta}{\mu_M} + \frac{\mathcal{R}_F\epsilon\eta(1-\delta)}{\mu_S} - \frac{\delta(1+\beta F^*)}{\mu_M} - \frac{\eta(1-\delta)(1+\beta F^*)}{\mu_S}}.
\end{aligned}
$$

This expression corresponds to the equation (13) in section 2.2.4. By replacing $C(F^*)$ in the same way with the expressions proposed in Section 2.1.1 in $\sigma(F^*)$ (13), we obtain bifurcation diagrams of a shape similar to those described in Section 2.2.4.

D $\sigma(F^*)$ numerator study

The numerator of $\sigma(F^*)$ is expressed as follows:

$$\frac{\beta p\mu_F}{(1-p)\mu_M}(F^*)^2 + \left(\frac{p\mu_F(1-\mathcal{R}_F)}{(1-p)\mu_M} + \beta k\right)F^* + k,$$

which can be rewritten as:

$$\frac{k}{\mathcal{R}_F}\left(\mathcal{R}_M\left(\beta F^*\right)^2 + \left(\mathcal{R}_M + \mathcal{R}_F - \mathcal{R}_M\mathcal{R}_F\right)\left(\beta F^*\right) + \mathcal{R}_F\right).$$

It does not depend on residual fertility rates, unlike the denominator. The discriminant of the βF^* second order polynomial is:

$$
\begin{aligned}
\Delta &= \left(\mathcal{R}_M + \mathcal{R}_F - \mathcal{R}_M\mathcal{R}_F\right)^2 - 4\mathcal{R}_F\mathcal{R}_M,\\
&= \mathcal{R}_M^2 + \mathcal{R}_F^2 + \mathcal{R}_F^2\mathcal{R}_M^2 + 2\mathcal{R}_F\mathcal{R}_M - 2(\mathcal{R}_M + \mathcal{R}_F)\mathcal{R}_M\mathcal{R}_F - 4\mathcal{R}_F\mathcal{R}_M.
\end{aligned}
$$

Thus the discriminant is positive if and only if:

$$(\mathcal{R}_M - \mathcal{R}_F)^2 + \mathcal{R}_M^2\mathcal{R}_F^2 > 2\mathcal{R}_M\mathcal{R}_F(\mathcal{R}_M + \mathcal{R}_F). \tag{D.19}$$

Dividing by $\mathcal{R}_M^2\mathcal{R}_F^2$ yields:

$$\left(\frac{1}{\mathcal{R}_F} - \frac{1}{\mathcal{R}_M}\right)^2 + 1 > 2\left(\frac{1}{\mathcal{R}_F} + \frac{1}{\mathcal{R}_M}\right).$$

Taking the inverse and muliplying by 4 yields:

$$\frac{2}{\frac{1}{\mathcal{R}_F} + \frac{1}{\mathcal{R}_M}} > \frac{4}{\left(\frac{1}{\mathcal{R}_F} - \frac{1}{\mathcal{R}_M}\right)^2 + 1}, \tag{D.20}$$

that is a lower-bound to the harmonic mean of $\mathcal{R}_F$ and $\mathcal{R}_M$. Since $\mathcal{R}_F, \mathcal{R}_M > 1$, we have $0 < \frac{1}{\mathcal{R}_F}, \frac{1}{\mathcal{R}_M} < 1$, so that $-1 < \frac{1}{\mathcal{R}_F} - \frac{1}{\mathcal{R}_M} < 1$ and $1 \leq \left(\frac{1}{\mathcal{R}_F} - \frac{1}{\mathcal{R}_M}\right)^2 + 1 < 2$. It follows that $2 < \frac{4}{\left(\frac{1}{\mathcal{R}_F} - \frac{1}{\mathcal{R}_M}\right)^2 + 1} \leq 4$ so that (D.20) imposes that the harmonic mean is larger than 2, and is necessarily satisfied when the harmonic mean is larger than 4 (Fig. D.2).

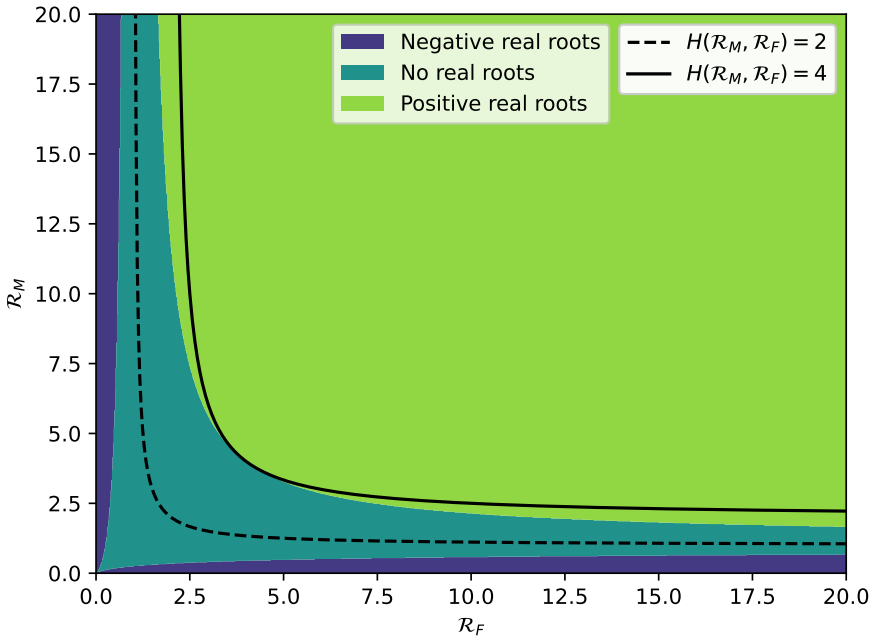

Figure D.2: Contour plot illustrating the existence of $\sigma(F^*)$ numerator roots as a function of the reproduction numbers $\mathcal{R}_M$ and $\mathcal{R}_F$. Three zones are defined: negative real roots (dark blue zone), no real roots (blue-green zone) and positive real roots (light green zone). The two curves represent the harmonic mean of $\mathcal{R}_M$ and $\mathcal{R}_F$ equal to 2 (dotted black curve) and equal to 4 (black curve).

In this case there are two roots. The product of the roots has the sign of $\frac{\mathcal{R}_F}{\mathcal{R}_M}$, which is positive. So the roots have the same sign.
The sum of the roots is:

$$-\frac{\mathcal{R}_M + \mathcal{R}_F - \mathcal{R}_M\mathcal{R}_F}{\mathcal{R}_M}. \tag{D.21}$$

Thus the sum of the roots is positive and therefore both roots are positive if and only if:

$$\begin{aligned} \mathcal{R}_F + \mathcal{R}_M < \mathcal{R}_M\mathcal{R}_F \quad &\iff \quad \tfrac{1}{\mathcal{R}_M} + \tfrac{1}{\mathcal{R}_F} < 1, \\ &\iff \quad \tfrac{2}{\frac{1}{\mathcal{R}_M} + \frac{1}{\mathcal{R}_F}} > 2. \end{aligned}$$

Hence, the harmonic mean of $\mathcal{R}_F$ and $\mathcal{R}_M$ must be larger than 2, which we have shown to be a consequence of equation (D.20). Hence, (D.19) or (D.20) suffice for the numerator to have two positive roots if $\mathcal{R}_F, \mathcal{R}_M > 1$ (Fig. D.2).

E Parameter values

E.1 Mortality rates

Different values for *Ceratitis capitata* lifespans were collected from the literature. The mortality rate was estimated as the inverse of the lifespan. Male and females lifespans and corresponding mortality rates are summarized in Table E.1.

Table E.1: *Ceratitis capitata* male and female lifespans based on the literature, with corresponding mortality rates.

References	Female lifespan (days)	Male lifespan (days)	μ_F (day^{-1})	μ_M (day^{-1})
Shoukry and Hafez (1979)	[25.5-31]	[25-36.5]	[0.032-0.039]	[0.027-0.040]
Carey (1984)	[39-46.4]	[40.5-47.9]	[0.022-0.026]	[0.021-0.025]
Vargas *et al.* (2000)	54.8	71.6	0.018	0.014
Papadopoulos *et al.* (2002)	21.1	29.5	0.047	0.034
Pieterse *et al.* (2020)	[12-17.5][1]	[17.6-35.5][2]	[0.057-0.083][1]	[0.036-0.057][2]

[1] Data extracted on nectarine and plum to collect extremum for females.
[2] Data extracted on apple and plum to collect extremum for males.

E.2 Emergence rate

The emergence rate r represents the mean number of eggs leading to the adult stage per female and per day. To estimate this parameter, data listed in Table E.2 were extracted from Pieterse *et al.* (2020). Only the values for nectarines were used, as they greatly vary between fruits and our aim was to make a rough estimate to calibrate the model. On average, females lay 25.75 eggs a day, 97% of which hatch in the fruits. Larvae then become pupae, 94.7% of which become adults. So, $r = 25.75 \times 0.97 \times 0.947 = 23.7$ day^{-1} with a range of values between 19.2 and 28.5 day^{-1}.

Table E.2: *C. capitata* development data extracted from Pieterse *et al.* (2020)

Fruit type	Eggs per females (24h)	Egg hatch in fruit (24h)	Pupal eclosion (24h)
Nectarine	25.75 [22.25-29.25]	97% [96%-98%]	94.7% [89.9%-99.5%]

E.3 Competition coefficient between females

The competition coefficient between females β represents oviposition competition. This parameter was estimated from the model without control by SIT at equilibrium. From equation (12), which allows us to find infestation equilibria of the model, we isolated β:

$$\begin{aligned} X(M(F))C(F) &= \frac{1}{\mathcal{R}_F}, \\ \frac{\frac{p\mu_F}{(1-p)\mu_M}F}{k+\frac{p\mu_F}{(1-p)\mu_M}F}\frac{1}{1+\beta F} &= \frac{1}{\mathcal{R}_F}, \\ 1+\beta F &= \frac{\mathcal{R}_F\frac{p\mu_F}{(1-p)\mu_M}F}{k+\frac{p\mu_F}{(1-p)\mu_M}F}, \\ \beta &= \frac{1}{F}\left(\frac{\mathcal{R}_F\frac{p\mu_F}{(1-p)\mu_M}F}{k+\frac{p\mu_F}{(1-p)\mu_M}F}-1\right). \end{aligned}$$

We based our estimate of females density F on several mass trapping studies (Demirel and Akyol, 2017; Hafsi *et al.*, 2020b; Leza *et al.*, 2008; Martinez-Ferrer *et al.*, 2012), in which about 1,000 females per day and per hectare were captured, assuming a balanced sex-ratio. We assumed that these traps captured most individuals and gave an approximation of *C. capitata* equilibrium density without SIT. Thus, taking $F = 1000$ ind.ha^{-1} and the parameter values listed in the Table 1, we obtain $\beta = 0.24$ (ind.ha^{-1})$^{-1}$.

Funding sources

The authors acknowledge the financial support of the CeraTIS - Corse project, within the framework of ECOPHYTO 2019, "Leviers territoriaux pour réduire l'utilisation et les risques liés aux produits phytopharmaceutiques (2020 - 2023)". M. Courtois's PhD is funded by INRAE.

References

Abram, P. K., Labbe, R. M., and Mason, P. G. (2021). Ranking the host range of biological control agents with quantitative metrics of taxonomic specificity. *Biological Control*, 152:104427.

Arita, L. and Kaneshiro, K. (1985). The dynamics of the lek system and mating success in males of the Mediterranean fruit fly, *Ceratitis capitata* (Wiedemann). *Hawaiian Entomological Society*, 25:39–48.

Aronna, M. S. and Dumont, Y. (2020). On nonlinear pest/vector control via the Sterile Insect Technique: impact of residual fertility. *Bulletin of Mathematical Biology*, 82(8):110.

Bakri, A. and Mehta, K. (2005). Sterilizing insects with ionizing radiation. *In: Dyck V, Hendrichs J, Robinson A, editors. Sterile Insect Technique. Springer*, pages 233–68.

Benedict, M. Q. (2021). Sterile Insect Technique: lessons from the past. *Journal of Medical Entomology*, 58(5):1974–1979.

Benedict, M. Q., Charlwood, J. D., Harrington, L. C., Lounibos, L. P., Reisen, W. K., and Tabachnick, W. J. (2018). Guidance for evaluating the safety of experimental releases of mosquitoes, emphasizing mark-release-recapture techniques. *Vector-Borne and Zoonotic Diseases*, 18(1):39–48.

Bliman, P.-A., Cardona-Salgado, D., Dumont, Y., and Vasilieva, O. (2019). Implementation of control strategies for Sterile Insect Techniques. *Mathematical Biosciences*, 314:43–60.

Caceres, C. (2002). Mass rearing of temperature sensitive genetic sexing strains in the Mediterranean fruit fly (*Ceratitis capitata*). *Genetica*, 116(1):107–116.

Carey, J. R. (1982). Demography and population dynamics of the Mediterranean fruit fly. *Ecological Modelling*, 16(2-4):125–150.

Carey, J. R. (1984). Host-specific demographic studies of the Mediterranean fruit fly *Ceratitis capitata*. *Ecological Entomology*, 9(3):261–270.

David, A. S., Kaser, J. M., Morey, A. C., Roth, A. M., and Andow, D. A. (2013). Release of genetically engineered insects: a framework to identify potential ecological effects. *Ecology and Evolution*, 3(11):4000–4015.

Demirel, N. and Akyol, E. (2017). Evaluation of mass trapping for control of Mediterranean fruit fly, *Ceratitis capitata* (Wiedemann) (Diptera: Tephritidae) in satsuma mandarin in Hatay province of Turkey. *International Journal of Environmental & Agriculture Research (IJOEAR)*, 3(12):32–37.

Duarte, F., Caro, A., Delgado, S., Asfennato, A., López, L., Hernández, F., and Calvo, M. V. (2022). Sterile Insect Technique (SIT) effectiveness to control *Ceratitis capitata* (Diptera: Tephritidae) and medfly catches in two mass trapping layouts. *International Journal of Pest Management*, 68(4):402–413.

Dumont, Y. and Oliva, C. F. (2023). On the impact of re-mating and residual fertility on the Sterile Insect Technique efficacy: case study with the medfly, *Ceratitis capitata*. preprint, Ecology.

Dunn, D. W. and Follett, P. A. (2017). The Sterile Insect Technique (SIT) – an introduction. *Entomologia Experimentalis et Applicata*, 164(3):151–154.

Dyck, V. A., Hendrichs, J., and Robinson, A. S., editors (2005). *Sterile Insect Technique: principles and practice in area-wide integrated pest management*. Springer, Dordrecht, Netherlands.

Dyck, V. A., Hendrichs, J., and Robinson, A. S. (2021). *Sterile Insect Technique: principles and practice in area-wide integrated pest management*. CRC Press, Boca Raton, 2 edition.

Eilenberg, J., Hajek, A., and Lomer, C. (2001). Suggestions for unifying the terminology in biological control. *BioControl*, 46(4):387–400.

Enkerlin, W., Gutiérrez Ruelas, J., Pantaleon, R., Soto Litera, C., Villaseñor Cortés, A., Zavala López, J., Orozco Dávila, D., Montoya Gerardo, P., Silva Villarreal, L., Cotoc Roldán, E., Hernández López, F., Arenas Castillo, A., Castellanos Dominguez, D., Valle Mora, A., Rendón Arana, P., Cáceres Barrios, C., Midgarden, D., Villatoro Villatoro, C., Lira Prera, E., Zelaya Estradé, O., Castañeda Aldana, R., López Culajay, J., Ramírez Y Ramírez, F., Liedo Fernández, P., Ortíz Moreno, G., Reyes Flores, J., and Hendrichs, J. (2017). The Moscamed Regional Programme: review of a success story of area-wide Sterile Insect Technique application. *Entomologia Experimentalis et Applicata*, 164(3):188–203.

Estal, P. D., Viñuela, E., Page, E., and Camacho, C. (1986). Lethal effects of microwaves on *Ceratitis capitata* Wied. (Dipt., Trypetidae). *Journal of Applied Entomology*, 102(1-5):245–253.

FAO/IAEA/USDA (2003). Manual for product quality control and shipping procedures for sterile mass-reared tephritid fruit flies.

Guerfali, M. M., Parker, A., Fadhl, S., Hemdane, H., Raies, A., and Chevrier, C. (2011). Fitness and reproductive potential of irradiated mass-reared Mediterranean fruit fly males *Ceratitis capitata* (Diptera: Tephritidae): lowering radiation doses. *Florida Entomologist*, 94(4):1042–1050.

Hafsi, A., Abbes, K., Harbi, A., and Chermiti, B. (2020a). Field efficacy of commercial food attractants for *Ceratitis capitata* (Diptera: Tephritidae) mass trapping and their impacts on non-target organisms in peach orchards. *Crop Protection*, 128:104989.

Hafsi, A., Rahmouni, R., Ben Othman, S., Abbes, K., Elimem, M., and Chermiti, B. (2020b). Mass trapping and bait station techniques as alternative methods for IPM of *Ceratitis capitata* Wiedmann (Diptera: Tephritidae) in citrus orchards. *Oriental Insects*, 54(2):285–298.

Hastings, A. and Gross, L. J., editors (2012). *Encyclopedia of theoretical ecology*. Number 4 in Encyclopedias of the natural world. University of California Press, Berkeley.

Hoffmann, A. A. and Ross, P. A. (2018). Rates and patterns of laboratory adaptation in (mostly) insects. *Journal of Economic Entomology*, 111(2):501–509.

Hooper, G. H. S. (1971). Competitiveness of gamma-sterilized males of the Mediterranean fruit fly: effect of irradiating pupal or adult stage and of irraditing pupae in Nitrogen1. *Journal of Economic Entomology*, 64(6):1364–1368.

Juan-Blasco, M., Sabater-Muñoz, B., Argilés, R., Jacas, J. A., Ortego, F., and Urbaneja, A. (2013). Effects of pesticides used on citrus grown in Spain on the mortality of *Ceratitis capitata* (Diptera: Tephritidae) Vienna-8 Strain Sterile Males. *Journal of Economic Entomology*, 106(3):1226–1233.

Kapranas, A., Collatz, J., Michaelakis, A., and Milonas, P. (2022). Review of the role of Sterile Insect Technique within biologically-based pest control – An appraisal of existing regulatory frameworks. *Entomologia Experimentalis et Applicata*, 170(5):385–393.

Klassen, W. and Creech, J. F. (1971). Suppression of pest population with sterile male insects. *Miscellaneous Publication*, 1182:2–8. USDA/ARS, Washington, DC, USA.

Klassen, W., Curtis, C., and Hendrichs, J. (2021). History of the Sterile Insect Technique. In *Sterile insect technique*, pages 1–44. CRC Press.

Klassen, W. and Vreysen, M. (2021). Area-wide integrated pest management and the Sterile Insect Technique. In *Sterile insect technique*, pages 75–112. CRC Press.

Knipling, E. F. (1955). Possibilities of insect control or eradication through the use of sexually sterile males. *Journal of Economic Entomology*, 48(4):459–462.

Leza, M. M., Juan, A., Capllonch, M., and Alemany, A. (2008). Female-biased mass trapping vs. bait application techniques against the Mediterranean fruit fly, *Ceratitis capitata* (Dipt., Tephritidae). *Journal of Applied Entomology*, 132(9-10):753–761.

Lynch, L. D. and Thomas, M. B. (2000). Nontarget effects in the biocontrol of insects with insects, nematodes and microbial agents: the evidence. *Biocontrol News and Information*, 21(4).

Magaña, C., Hernández-Crespo, P., Ortego, F., and Castañera, P. (2007). Resistance to Malathion in field populations of *Ceratitis capitata*. *Journal of Economic Entomology*, 100(6):1836–1843.

Manoukis, N. C. and Hoffman, K. (2014). An agent-based simulation of extirpation of *Ceratitis capitata* applied to invasions in California. *Journal of Pest Science*, 87(1):39–51.

Martinez-Ferrer, M. T., Campos, J. M., and Fibla, J. M. (2012). Field efficacy of *Ceratitis capitata* (Diptera: Tephritidae) mass trapping technique on clementine groves in Spain. *Journal of Applied Entomology*, 136(3):181–190.

Melvin, R. and Bushland, R. (1936). A method of rearing *Cochliomyia americana* C and P on artificial media. *US Department of Agriculture, Bureau of Entomology and Plant Quarantine.*

Messoussi, S. E., Hafid, H., Lahrouni, A., and Afif, M. (2007). Simulation of temperature effect on the population dynamic of the Mediterranean fruit fly *Ceratitis capitata* (Diptera; Tephritidae). *Journal of Agronomy*, 6(2):374–377.

Morelli, R., Paranhos, B. J., Coelho, A. M., Castro, R., Garziera, L., Lopes, F., and Bento, J. M. S. (2013). Exposure of sterile Mediterranean fruit fly (Diptera: Tephritidae) males to ginger root oil reduces female remating: ginger root oil reduced remating in wild medfly females. *Journal of Applied Entomology*, 137:75–82.

Odarc (2022). Office du développement agricole et rural de corse, chiffres clés de l'agriculture corse. https://www.odarc.corsica/attachment/2442561/.

Oliva, C., Mouton, L., Colinet, H., Debelle, A., Gibert, P., and Fellous, S. (2022). Sterile Insect Technique: Principles, Deployment and Prospects. In Fauvergue, X., Rusch, A., Barret, M., Bardin, M., Jacquin-Joly, E., Malausa, T., and Lannou, C., editors, *Extended Biocontrol*, pages 55–67. Springer Netherlands, Dordrecht.

Oliva, C. F., Benedict, M. Q., Collins, C. M., Baldet, T., Bellini, R., Bossin, H., Bouyer, J., Corbel, V., Facchinelli, L., Fouque, F., Geier, M., Michaelakis, A., Roiz, D., Simard, F., Tur, C., and Gouagna, L.-C. (2021). Sterile Insect Technique (SIT) against Aedes species mosquitoes: a roadmap and good practice framework for designing, implementing and evaluating pilot field trials. *Insects*, 12(3):191.

Papadopoulos, N. T., Carey, J. R., Liedo, P., Müller, H.-G., and Sentürk, D. (2009). Virgin females compete for mates in the male lekking species *Ceratitis capitata*. *Physiological Entomology*, 34(3):238–245.

Papadopoulos, N. T., Katsoyannos, B. I., and Carey, J. R. (2002). Demographic parameters of the Mediterranean fruit fly (Diptera: Tephritidae) reared in apples. *Annals of the Entomological Society of America*, 95(5):564–569.

Parker, A. and Mehta, K. (2007). Sterile Insect Technique: a model for dose optimization for improved sterile insect quality. *Florida Entomologist*, 90(1):88–95.

Pieterse, W., Manrakhan, A., Terblanche, J. S., and Addison, P. (2020). Comparative demography of *Bactrocera dorsalis* (Hendel) and *Ceratitis capitata* (Wiedemann) (Diptera: Tephritidae) on deciduous fruit. *Bulletin of Entomological Research*, 110(2):185–194.

Prokopy, R. J. and Hendrichs, J. (1979). Mating behavior of *Ceratitis capitata* on a field-caged host tree. *Annals of the Entomological Society of America*, 72(5):642–648.

Ramírez-Santos, E. M., Rendón, P., Ruiz-Montoya, L., Toledo, J., and Liedo, P. (2016). Performance of a genetically modified strain of the Mediterranean fruit fly (Diptera: Tephritidae) for area-wide integrated pest management with the Sterile Insect Technique. *Journal of Economic Entomology*, page tow239.

Robinson, A. (2002). Genetic sexing strains in Medfly, *Ceratitis capitata*, Sterile Insect Technique programmes. *Genetica*, 116(1):5–13.

Robinson, A. (2005). Genetic basis of the Sterile Insect Technique. *In: Dyck V, Hendrichs J, Robinson A, editors. Sterile Insect Technique. Springer*, pages 95–114.

Robinson, A. S., Cayol, J. P., and Hendrichs, J. (2002). Recent findings on medfly sexual behavior: implications for SIT. *Florida Entomologist*, 85(1):171–181.

Robinson, A. S. and Hooper, G. (1989). *Fruit flies: their biology, natural enemies and control*. Number 3A-3B in World crop pests. Elsevier, Amsterdam Oxford New York.

Sancho, R., Guillem-Amat, A., López-Errasquín, E., Sánchez, L., Ortego, F., and Hernández-Crespo, P. (2021). Genetic analysis of medfly populations in an area of Sterile Insect Technique applications. *Journal of Pest Science*, 94(4):1277–1290.

Serebrovsky, A. (1940). On the possibility of a new method for the control of insect pests. *Zoologicheskii Zhurnal*, 19:618–630.

Shelly, T. and McInnis, D. (2016). Sterile Insect Technique and control of Tephritid fruit flies: do species with complex courtship require higher overflooding ratios? *Annals of the Entomological Society of America*, 109(1):1–11.

Shoukry, A. and Hafez, M. (1979). Studies on the biology of the Mediterranean fruit fly *Ceratitis capitata*. *Entomologia Experimentalis et Applicata*, 26(1):33–39.

Sobol, I. (1990). On sensitivity estimates for nonlinear mathematical models. *Matematicheskoe modelirovanie*, 2(1):112–118.

Turgeon, J., Tayeh, A., Facon, B., Lombaert, E., De Clercq, P., Berkvens, N., Lundgren, J. G., and Estoup, A. (2011). Experimental evidence for the phenotypic impact of admixture between wild and biocontrol Asian ladybird (*Harmonia axyridis*) involved in the European invasion. *Journal of Evolutionary Biology*, 24(5):1044–1052.

Vargas, R. I., Walsh, W. A., Kanehisa, D., Stark, J. D., and Nishida, T. (2000). Comparative demography of three Hawaiian fruit flies (Diptera: Tephritidae) at alternating temperatures. *Annals of the Entomological Society of America*, 93(1):75–81.

Vreysen, M., Hendrichs, J., and Enkerlin, W. (2006). The Sterile Insect Technique as a component of sustainable area-wide integrated pest management of selected horticultural insect pests. *Journal of Fruit and Ornamental Plant Research*, 14:107–132.

Whittier, T. S., Kaneshiro, K. Y., and Prescott, L. D. (1992). Mating behavior of Mediterranean fruit flies (Diptera: Tephritidae) in a natural environment. *Annals of the Entomological Society of America*, 85(2):214–218.

Wu, J., Dhingra, R., Gambhir, M., and Remais, J. V. (2013). Sensitivity analysis of infectious disease models: methods, advances and their application. *Journal of The Royal Society Interface*, 10(86):20121018.

Zavala-López, J. and Enkerlin, W. (2017). (FAO/IAEA) Food and Agriculture Organization of the United Nations/International Atomic Energy Agency. Guideline for packing, shipping, holding and release of sterile flies in area-wide fruit fly control programmes. Second edition.